Published in final edited form as:
Dev Neurobiol. 2012 April ; 72(4): 628–648. doi:10.1002/dneu.20967.

Dynamic responses of *Xenopus* retinal ganglion cell axon growth cones to netrin-1 as they innervate their *in vivo* target

Nicole J. Shirkey[1], **Colleen Manitt**[1], **Liliana Zuniga**, and **Susana Cohen-Cory**[*]
Department of Neurobiology and Behavior, University of California Irvine, Irvine CA 92697, USA.

Abstract

Netrin-1 influences retinal ganglion cell (RGC) axon pathfinding and also participates in the branching and synaptic differentiation of mature RGC axons at their target. To investigate whether netrin also serves as an early target recognition signal in the brain, we examined the dynamic behavior of *Xenopus* RGC axons soon after they innervate the optic tectum. Time-lapse confocal microscopy imaging of RGC axons expressing EYFP demonstrated that netrin-1 is involved in early axon branching, as recombinant netrin-1 halted further advancement of growth cones into the tectum and induced back branching. RGC growth cones exhibited differential responses to netrin-1 that depended on the degree of differentiation of the axon and the developmental stage of the tadpole. Netrin-1 decreased the total number of branches on newly arrived RGC growth cones at the target, but increased the dynamic branching of more mature arbors at the later developmental stage. To further explore the response of axonal growth cones to netrin, *Xenopus* RGC axons were followed in culture by time-lapse imaging. Exposure to netrin-1 rapidly increased the forward advancement of the axon and decreased the size and expanse of the growth cone, while also inducing back branching. Taken together, the differential *in vivo* and *in vitro* responses to netrin-1 suggest that netrin alone is not sufficient to induce the cessation of growth cone advancement in the absence of a target, but can independently modulate axon branching. Collectively, our findings reveal a novel role for netrin on RGC axon branch initiation as growth cones innervate their target.

Keywords

Retinal ganglion cell; *in vivo* imaging; netrin; axon; growth cone; *Xenopus laevis*

Axon targeting and branch initiation are crucial steps in the formation of neuronal connections during development. Long projecting axons, directed by growth cones at their leading edge, must recognize their appropriate final target to begin arborizing and to establish functional synaptic connections. Growth cone pathfinding is directed by molecular cues along the pathway and at intermediate choice points. Upon arriving at their final targets, axonal growth cones switch from a pathfinding program to one of axon arbor branching and synaptic differentiation. Axon branching at the target is known to occur primarily by the formation of collateral branches along the axon shaft behind the leading growth cone, a mechanism known as back branching (Harris et al., 1987; Davenport et al., 1999). Accumulating evidence indicates that molecular cues that can guide axons to their target can also participate in the induction of back branching following target innervation (Brose et al., 1999; Wang et al., 1999; Brose and Tessier-Lavigne, 2000; Campbell et al., 2001). The cellular and molecular mechanisms underlying the transition from axon

[*]Corresponding Author: Susana Cohen-Cory, Ph.D., Department of Neurobiology and Behavior, University of California, Irvine, 2205 McGaugh Hall, Irvine, CA 92697-4550, phone: (949)824-8188, Fax:(949) 824-2447, scohenco@uci.edu.
[1]Indicates equal contribution.

pathfinding to target recognition and axon branch initiation, especially in an *in vivo* context, are not yet well understood.

The *Xenopus laevis* visual system has been used as an experimental model to provide important insights into the formation of neuronal connections during development, including axon guidance, targeting, arborization and synaptogenesis. In *Xenopus*, the bi-directional guidance cue netrin-1 has been shown to modulate several aspects of retinotectal circuit formation in a developmentally-dependent manner. Netrin functions as an attractive cue that guides RGC axons out of the eye and into the optic nerve through activation of one of its receptors, deleted-in-colorectal-cancer (DCC) (de la Torre et al., 1997; Deiner et al., 1997; Hopker et al., 1999). Although netrin is expressed at the optic chiasm and in the ventral optic tectum, evidence from a semi-intact optic pathway preparation in culture shows that RGC growth cones are non-responsive to netrin-1 at the developmental stage when they enter the brain and decussate at the optic chiasm, but at the stage they approach the target optic tectum they are repelled by netrin-1 (Shewan et al., 2002). Thus RGC growth cones switch their response from attraction, to neutral, to repulsion as they navigate along their pathway. In addition to a role in axon pathfinding, recent evidence demonstrates that netrin-1 participates in the synaptic maturation and arborization of RGC axons already actively branching in the optic tectum (Manitt et al., 2009). Together, these studies suggest that netrin-1 may also participate as an early target-derived signal for newly arborizing RGC axons in the brain.

Here we tested the hypothesis that netrin is involved in branch initiation responses of newly targeted RGC axon growth cones in the optic tectum. Axon targeting and branch initiation by *Xenopus* RGC axon growth cones was examined at two developmental stages that correspond to distinctive periods of retinotectal circuit development. An early stage (stage 40) when RGC axons first innervate the optic tectum and are beginning to form functional connections, and a later developmental stage (stage 45) during which extensive axon arborization and synapse formation are underway while late projecting RGC axons continue to innervate their in vivo target. Time-lapse imaging of RGC growth cones expressing EYFP demonstrated that alterations in netrin-1 signaling influence early axon branch dynamics and growth. Microinjection of netrin-1 halted the further advancement of newly targeted RGC growth cones into the optic tectum and induced back branching. Moreover, time-lapse imaging showed that RGC growth cones exhibit differential responses to netrin-1 that depend on the developmental stage of the tadpole and the degree of differentiation of the axon. The response of RGC axon growth cones to netrin-1 was also examined in culture following application of varying concentrations of netrin by time-lapse DIC imaging. Differential *in vivo* and *in vitro* responses to netrin-1 indicate that netrin can independently induce back branching, but that it is not sufficient to induce the cessation of growth cone advancement in the absence of a target.

Materials and Methods

Xenopus laevis tadpoles were obtained by *in vitro* fertilization of oocytes from adult females primed with human chorionic gonadotropin. Tadpoles were raised in rearing solution (60 mM NaCl, 0.67 mM KCl, 0.34 mM $Ca(NO_3)_2$, 0.83 mM $MgSO_4$, 10 mM HEPES pH 7.4, 40 mg/l gentamycin) with 0.001% phenylthiocarbamide to prevent melanocyte pigmentation. Tadpoles were anesthetized during experimental manipulations in 0.05% tricane methanesulfonate (Finquel, Argent Laboratories), and were allowed to swim freely in rearing solution between imaging sessions. Staging was done according to Nieuwkoop and Faber (Nieuwkoop and Faber, 1956). Animal procedures were approved by the University of California, Irvine.

RGC axon labeling and in vivo time-lapse imaging

To visualize RGC growth cones *in vivo*, *Xenopus* embryos were lipofected in one eye with enhanced yellow fluorescent protein (EYFP) expression vectors. Transfection and *in vivo* imaging of RGCs was performed as described previously (Alsina et al, 2001). Briefly, DNA plasmids encoding EYFP (Clontech) were transfected into the eye primordium of stage 20–22 tadpoles by lipofection with DOTAP liposomal transfection reagent (Roche Diagnostics). Tadpoles were left to develop until either stage 39/40 or stage 45, and then screened for individual EYFP-expressing RGC axons in the optic tectum. The morphological behavior of fluorescently labeled RGC axons was followed by confocal microscopy in tadpoles at the two different stages of development and at two distinct morphological differentiation states of the arbor within these stages. Only animals with 1–2 labeled RGC axons were used for imaging. For analysis of newly targeted RGC axons, tadpoles with single EYFP-expressing RGC axons exhibiting a simple (less than 12 processes), undifferentiated morphology with a growth cone at their leading tip were selected for experimentation and imaging. For the analysis of branched arbors, tadpoles with EYFP-expressing RGC axon arbors with more than 17 branches and without a growth cone were selected and used for experimentation and imaging. For all groups, tadpoles were imaged every two hours for 6 to 8 hours and then again at 24 hours. Confocal images were acquired as described previously (Hu et al, 2005). Briefly, thin optical sections (1.5 μm) through the entire extent of the arbor were collected at 60x magnification (1.00 NA water-immersion objective) with a Nikon PCM2000 laser-scanning confocal microscope. Images were obtained below saturation levels, with minimal gain and contrast enhancement. Immediately after the first imaging (time 0), 0.2–1.0 nl of recombinant chicken netrin-1 (300 ng/μl; R&D Systems), anti-DCC (330 ng/μl; AF5, Calbiochem (Hong et al., 1999), or vehicle solution (0.1% BSA in PBS) was pressure injected into the ventricle and subpial space overlying the optic tectum. As in previous studies, axons of vehicle-injected control tadpoles show comparable branch morphologies to tadpoles injected with non-immune mouse IgG (300 ng/μl) (Manitt et al, 2009).

Data analysis

All analysis was performed from raw confocal images without any post acquisition manipulation or thresholding as described previously (Alsina et al., 2001; Hu et al., 2005; Marshak et al., 2007). Analysis was performed blind to the treatment group. Digital three-dimensional reconstructions of EYFP labeled axons were obtained from individual optical sections through the entire extent of the arbor with the aid of MetaMorph software. To determine growth cone advancement within the target, we measured the forward migration of each growth cone using intrinsic axon landmarks (bends in the axon and identifiable branches). Morphological landmarks that remained stable across time points for each individual axon also allowed identification of stable, added, and eliminated branches from one observation time point to the next. For the quantitative analysis of axon branching, total arbor branch length (length of total branches), total branch number, the number of individual branches added, and the number of branches remaining from one observation interval to the next, were measured. To determine forward and back-branching for each axon, individual 3-D reconstructions of time-lapse images were aligned using branches and curvatures in the axon that were common to all time-points (see for example Figure 1 A, B white arrows in top panels and Fig. 2A asterisks and black arrows). Landmarks along the axon were also used to draw a reference line below the growth cone location (at about 10 μm from the growth cone base) in the axon at time 0 (see Fig. 1 A, B as examples; horizontal line). Axon branches above (forward) or below (back) the original position of the growth cone at the tip of the axon were identified and counted. Thus, for this measurement, “forward branches” corresponded to processes formed on newly extended segments of the axon shaft as the growth cone advanced relative to the location of its leading edge at time 0, and “back branches” corresponded to branches or processes that formed on the axon segment behind

the growth cone's position at time 0. Reconstructions of each individual axon were also used to determine whether the axon "shortened", "lengthened", or remained the "same" by 24 hours relative to time 0 (just prior to treatment). A total of 20 axons for control, 18 for netrin and 14 for anti-DCC treatment were analyzed, with one axon analyzed per tadpole. Data are presented as either net or percent change from the initial value for each individual axon, or as the change between two observation intervals for each individual axon. Two-sample unpaired *t*-tests were used for the statistical analysis of data (Graph-Pad Prism software). Results were classified as significant as follows: $*p \leq 0.05$, $**p \leq 0.005$, $***p \leq 0.0005$.

Eye explant cultures

Eye explants from stage 25 *Xenopus* tadpoles were cultured as previously described (Harris et al, 1985; Harris & Massersmith, 1992). Eyebuds were plated in 60% L-15 media containing 1% fungibact (UCSD Core) and 0.1% fatty acid free BSA (Sigma) on fibronectin (Sigma) coated poly-d-lysine substrates (MatTek Corporation). Cultures were grown for 24 hours in a humidified incubator at room temperature (20°C), and then imaged using an Axiovert 200 inverted microscope (Zeiss). For all axons, differential interference contrast images from one growth cone per culture dish were captured once every 30 seconds for 1 hour with a digital camera (Zeiss) with a 63x objective. Growth cones at the tip of axons without any detectable fasciculation, which did not overlap with other growth cones or axons, and presented characteristic growth cone morphology, were selected for imaging. Images were processed using MetaMorph software. After an initial five minutes of imaging for baseline comparisons, cultures were treated with either vehicle (0.1% BSA in PBS) or one of three concentrations of recombinant chicken netrin (10 ng/ml, 100 ng/ml, or 300 ng/ml) by bath application.

Immunostaining and imaging of explant cultures

Immediately following imaging, all cultures were fixed for one hour with 4% PFA with 7.5% sucrose and then washed with PBS. Cultures were incubated for 15 minutes with 0.2% TritonX-100 in PBS, rinsed with PBS, incubated with rhodamine-phalloidin (1:100 dilution; Molecular Probes), then washed again with 0.2% Triton X-100 in PBS. Following the phalloidin staining, cultures were incubated for 30 minutes at room temperature in blocking solution (2% bovine serum albumin and 0.2% TritonX-100 in PBS), and immunostained with antibodies against the presynaptic protein SNAP-25 (1:1,000 dilution; Stressgen Bioreagents Corporation) or the netrin receptor DCC (BD Pharmingen) in blocking solution for 24 hours at 4°C. Primary antibodies to DCC, either directed against the intracellular domain of DCC or against the extracellular domain (both from BD Pharmingen) were used at a 1:3,000 dilution. Immunostaining patterns, and effects of netrin on DCC immunostaining were comparable when using either of the two anti-DCC antibodies (data not shown). Primary antibodies were visualized using a goat anti-mouse Alexa 488 secondary antibody (1:1,000 dilution for SNAP-24, 1:2,000 for both DCC antibodies; Invitrogen). Fluorescent images were captured, using the same exposure time and gain settings for all samples, using an Axiovert 200 inverted microscope (Zeiss), and processed using MetaMorph software. To quantify differences in immunostaining, fluorescent images (SNAP-25 or DCC immunolabel) were thresholded and binarized, and the number of labeled pixels in an average of 100 μm of axon length were determined with the aid of MetaMorph software.

Analysis of RGC growth cones in culture

Data obtained both from time-lapse imaged axons, and from axons imaged after fixation, were analyzed using MetaMorph software. Parameters examined per individual axon were: area of the growth cone, area encompassing growth cone filopodia, total length of all processes including the axon shaft, number of growth cone processes, and the number of

processes behind the growth cone (more than 1.5 μm). Forward growth of the axon (change in length relative to time 0) was also evaluated for axons followed by time lapse imaging. Data are presented as either net or percent change from the initial value at time 0 for each individual axon, or as the change between two observation intervals as indicated. Two-sample unpaired t-tests were used for the statistical analysis of data (GraphPad Prism software). Results were classified as significant as follows: *$p \leq 0.05$, **$p \leq 0.005$, ***$p \leq 0.0005$.

Results

In the presence of netrin-1, RGC growth cones halt their advancement within their *in vivo* target

Our previous work demonstrates that in addition to being involved in RGC axon pathfinding, netrin-1 induces the formation of presynaptic specializations and influences branching dynamics in axons actively arborizing in their brain target, the optic tectum (Manitt et al, 2009). To test whether netrin is also involved in early RGC axon targeting events, we analyzed growth cone migration within the target and early branching responses of EYFP-expressing RGC axon growth cones in stage 40 *Xenopus laevis* tadpoles. Growth cone morphologies of RGC axons at this developmental stage were variable, ranging from growth cones displaying broad/large lamellipodia to growth cones displaying a narrow or slender morphology at their tip (see Figs. 1 A, B and 4 A for representative examples). Our analysis revealed that within 24 hours following microinjection of recombinant netrin-1 into the tadpole optic tectum, axons in netrin-treated tadpoles exhibited significantly less forward advancement than controls (change in length from 0 to 24 hours: netrin −7.36 ± 9.35 μm, control 29.19 ± 13.37 μm; $p = 0.03$) (Fig. 1 A–C). Counting the number of axons that shortened, lengthened, or remained the same length revealed that the majority of axons in control-treated tadpoles lengthened over the 24 hour observation period (80%; n = 20), while only 22% in netrin-treated tadpoles showed continued forward growth (n=18) (Fig. 1 A–B, D). Although growth cones initially advanced from their location at time 0 within the optic tectum, by the end of the 24 hr observation period the majority of axons in control tadpoles had ceased to continue their forward growth. This suggests that within this time period, control RGC axons had reached their appropriate topographical location within the target optic tectum (data not shown). Evidence that supports this interpretation is revealed by the arborization patterns of control axons at the 24 hr time point (see control axons in Fig. 1 A), where growth cone structures were no longer observed, and the axon had assumed a moderate degree of arborization.

Netrin influences branch initiation in RGC axon growth cones at the target

To further examine the effects of netrin on RGC axons at the target, we determined the change in total branch number at each observation time point relative to the number of branches present at time 0. By 24 hours following treatment, axons in netrin-treated tadpoles increased their total branch number significantly less than controls. The total branch number of simple growth cone containing axons in netrin-treated tadpoles increased by only 1.69 ± 0.75 branches between 0 and 24 hours, while in controls there were 8.88 ± 1.40 more branches over the 24 hr period ($p = 0.0001$) (Fig. 1 E). A measure of the absolute change in total arbor length (combined length of all branches and axon shaft) also revealed that netrin treatment significantly influenced arbor growth, as the change in total arbor length of axons in netrin-treated tadpoles was less than 50% of the increase observed in controls by 24 hours post-treatment (control: 94.49 ± 18.18 μm from 0–24 hrs; netrin: 40.93 ± 16.36 μm from 0–24 hrs, $p = 0.04$). It is important to note that while growth cones exposed to netrin-1 possessed significantly fewer total branches than controls by 24 hours (total branches at time 0: 8.05 ± 0.63 for control and 7.62 ± 0.69 for netrin; $p = 0.8$; total branches at 24 hrs: 16.82

± 1.35 for control and 9.22 ± 0.95 for netrin; $p = 0.0001$), they still significantly increased their total arbor length over the 24 hour period, indicating that in the presence of excess netrin, growth cones did continue to lengthen (netrin: 2.27 ± 6.53 μm from 0–2 hrs, 40.93 ± 16.36 μm from 0–24 hrs; $p = 0.03$) (Fig. 1 F). These results therefore suggest that while netrin impacts branch formation, it does not prevent the growth of existing branches.

Netrin induces back branching in RGC axon growth cones

The observation that netrin-1 interfered with forward growth suggested that acute netrin-1 treatment may precipitate the events that lead to the cessation of growth cone advancement within the target. Lateral extensions on RGC axons innervating the optic tectum in chick or superior colliculus in mouse form as axon growth cones collapse and retract after contacting inappropriate target neurons. This collapse event is correlated with nascent branch formation along the axon shaft and constitutes what is known as back branching (Davenport et al., 1996; Yates et al., 2001). In *Xenopus*, RGC axon growth cones do not retract, but are instead reported to slow, expand, and become more complex as they reach their targets. In *Xenopus*, lateral branching from the axon shaft occurs as the growth cone gradually disappears and assumes the morphology of a branch (Harris et al., 1987). Thus, to determine if netrin plays a role in early branch initiation, we quantified the number of branches present on the axon shaft behind the initial location of the growth cone ("back branches") and beyond the location of the growth cone ("forward branches") for each axon and assessed the change in forward- and back-branch number at each observation time point relative to time 0 (see schematic in Fig. 2 A). This analysis revealed that control axons significantly increase the number of forward branches over the 24 hour observation period (7.00 ± 1.30 branches; see Fig. 1 A and Fig. 2 B), indicating that the axons continued to extend along the target over time. Growth cones exposed to excess netrin-1, however, added very few branches beyond the initial location of their growth cone at all time intervals (0–2 hrs: 0.63 ± 0.37, 0–4 hrs: 0.47 ± 0.27, 0–6: 0.16 ± 0.19, and 0–24 hrs: 0.24 ± 0.38, Fig 2B). As a result, axons in netrin-treated tadpoles significantly differed in their forward branches when compared to control axons over the 24 hour observation period (control: 7.00 ± 1.30, netrin: 0.24 ± 0.38; $p < 0.001$, Fig 2B). This difference in forward branching between netrin and control treated axons was significant by four hours after treatment (control: 1.75 ± 0.43 branches, netrin: 0.47 ± 0.27 branches; $p = 0.02$) and was maintained over time (Fig. 2 B). Thus netrin interferes with the growth and extension of forward branches in newly arborizing RGC axons.

In contrast to the extension of new forward branches beyond the growth cone, control axons decreased their number of back branches within the first six hours of imaging (Fig 2D). This initial decrease in back branch number was transient, as axons exhibited a significant increase in back-branching by the end of the 24 hr observation period (Change in back branch number: −1.00 ± 0.38 for control 0–2 hrs, 1.94 ± 1.15 for control 0–24 hrs; $p = 0.014$; see Fig. 1 A and 2 D). This delayed increase in back branching in control axons is consistent with the observations that the majority of control growth cones continued to advance within the optic tectum between 0 and 6 hours, and that by the end of the 24 hour observation period all control axons had stopped advancing and exhibited a more complex morphology which was accompanied by the loss of their growth cone. In contrast to the early loss of back branches in controls, growth cones in netrin-treated tadpoles gradually increased the number of back branches (Change in back branch number: 0.05 ±0.39 at 0–2 hrs after netrin treatment, 1.35 ± 0.59 at 0–24 hrs after netrin treatment; $p = 0.07$; see Figs. 1 B and 2 D). Between two and four hours after the initial observation and treatment, growth cones in netrin-treated tadpoles extended, rather than pruned, significantly more back branches than axons in control tadpoles (Change in back branch number: -1.30 ± 0.62 at 0–4 hrs after control treatment, 0.53 ± 0.49 at 0–4hrs after netrin treatment; $p = 0.03$, Fig 2D),

suggesting that netrin-1 induced an early formation of back branches. The observation that the number of back branches in axons in controls versus netrin-treated tadpoles did not differ past the six hour observation is consistent with the idea that excess netrin induced back-branching earlier in time, but that the effect of netrin treatment was transient because control growth cones also began to extend back branches by the end of the observation period.

To obtain a correlate between forward branching and back branching, a ratio of these two branch categories was calculated for each imaging time point (Fig. 2C). A ratio value of 1 indicates that at that time point, axon branches were evenly distributed both beyond and behind the initial growth cone location, while a ratio less than 1 represents an arbor that extends more back branches than forward branches. Conversely, a ratio greater than 1 indicates that an axon extends relatively more forward than back branches as the growth cone advances. The pre-treatment baseline for both control and netrin-treated growth cones was similar for both groups at time 0 (forward-back branch ratio: 0.37 ± 0.09 for controls, 0.33 ± 0.10 for netrin, Fig 2C). This ratio significantly increased for controls to 1.45 ± 0.33 by 24 hours indicating that control axons significantly increased the proportion of forward relative to back branches as the growth cone advanced. Growth cones in the netrin-treated tadpoles, however, maintained a similar ratio over time (forward-back branch ratio: 0.32 ± 0.08 at 24 hrs, Fig 2C), consistent with our observation that growth cones tend to cease their advancement into the target following treatment with exogenous netrin-1. Due to the differences in forward versus back branching, axons in netrin-treated tadpoles became significantly different from axons in control tadpoles at 6 hours (forward-back branch ratio: 0.63 ± 0.12 at 6 hrs after control treatment, 0.33 ± 0.08 at 6 hrs after netrin treatment; $p = 0.05$, Fig 2C), a difference that persisted and became more significant over time (forward-back branch ratio: 1.45 ± 0.33 at 24 hrs after control treatment, 0.32 ± 0.08 at 24 hrs after netrin treatment; $p = 0.003$, Fig 2C).

RGC growth branch dynamics in the presence of excess netrin-1 at the target

To further determine the effects of increasing tectal netrin levels on early branch initiation and the branching patterns of RGC axons, we analyzed axon branch dynamics by following each branch from one observation time point to the next. We determined the number of branches newly added (added branches), and the number of branches that persisted (stable branches), between observation time points. Values for added and stable branches are presented as net changes that occurred every 2 hours in axons followed for six hours, and changes between 6 and 24 after treatment (Fig. 3). The analysis of branch dynamics showed that on average, control axons added 3.1 ± 0.33 branches in every 2 hr observation interval and 10.5 ± 1.2 branches between 6 and 24 hrs after initial imaging (Fig. 3A, see also Fig. 1 E). The number of stable branches in control axons remained the same throughout the 24 hour observation period (average 2 hour intervals; 6.18 ± 0.41 stable branches, and 6–24 hour interval; 6. 31 ± 0.68 stable branches; Fig 3B), indicating that axon arbors become more complex primarily by the addition of new branches and stabilization of existing branches. Branch dynamics following netrin treatment were similar to those in control axons early after treatment. Axons exposed to netrin-1 added a similar number of branches as controls every 2 hours (Added branches 3.1 ± 0.33 for control, 3.46 ± 0.27 for netrin; $p = 0.45$), and had a similar number of stable branches as controls (2 hr intervals: 6.18 ± 0.41 stable branches for control, 5.44 ± 0.29 for netrin ; $p = 0.19$). However, new branch addition was significantly lower in axons exposed to netrin-1 in the 6–24 hour observation interval (10.5 ± 1.2 branches for control, 3.81 ± 0.75 branches for netrin; $p = 0001$, Fig. 3A), while the number of stable branches (6.31 ± 0.68 for control, 6.50 ± 0.48 for netrin; $p = 0.82$, Fig. 3B) and the number of branches eliminated (3.875 ± 0.54 for control, 2.688 ± 0.53 for netrin, $p = 0.13$, not shown graphically) remained similar to controls. This indicates that

dynamic, netrin-1-induced changes in newly differentiating axon arbors are initially mediated by the extension of new branches which then slows down in the presence of excess netrin-1.

To establish whether changes in branch extension occur differentially along the axon, we analyzed branch dynamics for the forward and back branches independently in the newly targeted RGC axons. Counting the proportion of added versus stable revealed that significantly more new forward branches than back branches were extended in control axons every 2 hrs (added branches at 2 hr intervals: 39.30 ± 4.56% for forward branches, 24.80 ± 2.86% for back branches; $p = 0.008$; Fig. 3C). This supports the observation that control axons grow primarily by dynamically adding forward branches as the growth cone advances, as well as by stabilizing a few remaining branches that were not pruned behind the initial location of the growth cone (back branches) (Fig. 3C and Fig. 2 B, C). The dynamic behavior of axons exposed to netrin-1, in contrast, showed that branches are preferentially added and stabilized behind the initial location of the growth cone. In proportion, as many back as forward branches were added after netrin treatment (Fig. 3C), and significantly more back branches were added in the newly targeted axons exposed to netrin-1 than in controls (24.8 ± 2.86% for control, 37.73 ± 3.07% for netrin, $p = 0.0026$, Fig. 3C). In contrast to controls, however, significantly fewer forward branches were stabilized after netrin treatment (stable forward branches: 60.31 ± 5.13% for controls, 35.09 ± 5.64% for netrin, $p = 0.001$; Fig. 3C). Therefore, as the back portion of the arbor gained new branches, the more dynamic elimination of forward branches resulted in a net loss of branches in the forward portion of the arbor early after netrin treatment (as indicated by a Δ change of added + stabilized branches below 100%, Fig. 3C). Dynamic analysis of forward versus back branches between 6 and 24 after initial imaging showed that the addition and stabilization of forward and back branches in axons in netrin-treated tadpoles returned to a level similar to controls, although only control axons showed continued forward growth (Δ change of added + stabilized branches above 100%, Fig 3D). These results therefore indicate that acute changes in netrin-1 levels influence the growth cone's decision of where to terminate by preferentially inducing dynamic changes that favor branch addition in already extended portions of the axon (see Fig. 3 E for a diagrammatic summary of these results).

RGC axon growth cones *in vivo* show an age and morphology-dependent branching response to netrin

Previous studies from our laboratory show that netrin significantly induces presynaptic site differentiation and increases the branching of more mature RGC axon arbors in stage 45 tadpoles within 24 hours of treatment (Manitt et al, 2009; see Fig. 4). Our present studies show an opposite effect by acute netrin treatment on newly targeted RGC axons in the stage 40 tadpole optic tectum (Fig. 1 E). These opposing results raised the possibility that RGC axons respond differentially to netrin in an age- or axon maturation-dependent manner. Age-dependent responses to netrin-1 have been described in the pathfinding of *Xenopus* RGC growth cones in an *in vitro* preparation, where netrin exerts an attractive influence on growth cones exiting the retina and a repellent influence on growth cones poised to enter the optic tectum (Shewan et al, 2002). Here, we examined the effects of acute netrin treatment on two additional populations of RGC axons *in vivo*: 1) RGC axons from stage 40 tadpoles with a morphologically more differentiated arbor (arbors with more than 17 branches and no growth cones), and 2) simple growth cone-containing RGC axons in stage 45 tadpoles (see Fig. 4 A, B). Our analysis of RGC axons in control stage 40 and stage 45 tadpoles revealed that axon branching rates are consistent throughout the two developmental stages in the normal developing brain. Specifically, no significant difference was observed in the increase in total branch number in actively branching axons as they mature to become more elaborate in stage 40 when compared to stage 45 tadpoles (Fig. 4 C, D). Similarly, no difference in

branching rate was observed in recently targeted growth cones in stage 40 versus stage 45 tadpoles ("simple GCs") (Fig. 4 C, D). In contrast, axons exposed to netrin showed significant differences in their number of branches depending on their complexity and stage of the tadpole as they matured. Specifically, comparisons based on maturational state of the arbor showed that branched axons increased their total branch number significantly more than simple growth cones following netrin treatment in stage 40 (delta branch number: 6.14 ± 1.88 for branched axons, 1.69 ± 0.75 for simple growth cones; $p = 0.01$), as well as in stage 45 tadpoles (delta branch number: 28.50 ± 4.85 for branched axons, 6.89 ± 0.90 for simple growth cones; $p = 0.002$). Comparisons by developmental stage showed that simple, growth cone-containing axons increased their branch number significantly more in stage 45 than in younger, stage 40 tadpoles (stage 45 growth cones: 6.89 ± 0.90 branches, stage 40 growth cones 1.69 ± 0.75 branches; $p = 0.0003$). Similarly, branched axons in stage 45 tadpoles increased their branch numbers significantly more than branched axons at stage 40 (Fig. 4 C, D). Taken together, these data indicate a gradual change in response by RGC axons to netrin that depends on both the stage of the tadpole and the maturational state of the axon. Indeed, branched axons in stage 40 tadpoles did not differ in their rate of branch elaboration when compared to simple stage 45 growth cones, either in the presence or absence of excess netrin (Fig. 4 C, D), indicating that morphologically more mature RGC axons in stage 40 and RGC growth cones in stage 45 tadpoles are non-responsive to netrin-1 treatment. Further analysis of the time course of responses over a 24 hour period of growth cones in stage 45 tadpoles and in branched axons of stage 40 tadpoles exposed to netrin-1 showed no differences in the branching of forward or back branches versus controls at any of the time intervals, nor in the ratio of forward to back branching (data not shown). Therefore, responses to netrin shift from a branch attenuation response in axons that are most immature (stage 40 growth cones), to neutral as they begin to branch and development proceeds, then finally to a branch-promoting effect of netrin in the more elaborate and mature axon arbors. Thus, both the maturational state of the axon arbor and the developmental stage of the tadpole appear to influence the response of RGC axons to netrin treatment.

DCC-mediated signaling impacts RGC growth cone branching

To explore the potential contribution of the DCC receptor to the response of RGC axon growth cones to netrin-1, time-lapse imaging of labeled RGC axons was performed following injection of function blocking antibodies to DCC into the stage 40 tadpole optic tectum. Responses of RGC growth cones following anti-DCC treatment showed levels of forward growth and branching that were different from those of controls and growth cones in netrin-treated tadpoles. Specifically, when quantifying rostrocaudal advancement within the target, analysis of change in length showed that anti-DCC-treatment prevented growth cone advancement overall (29.19 ± 12.37 μm for control, −2.86 ± 14.06 μm for anti-DCC; $p = 0.10$) (Fig. 5 A). A smaller portion of growth cones lengthened over time following anti-DCC treatment (80% for control, 57% for anti-DCC) (Fig. 5 B). Moreover, growth cones in tadpoles treated with anti-DCC showed no net increase in branch number during the first six hours of imaging (Fig. 5 C), and had significantly lower increase in total branches than controls by 24 hours (8.88 ± 1.40 for control, 4.75 ± 1.36 for anti-DCC; $p = 0.05$; Fig. 5 C). The increase in forward branch number was significantly lower than controls 24 hours following anti-DCC treatment (7.00 ± 1.31 for control, 1.17 ± 0.37 for anti-DCC; $p = 0.001$; Fig. 5 D), but back branches changed at a rate similar to controls (Fig. 5 E). This difference in forward versus back branching resulted in growth cones exposed to anti-DCC exhibiting a forward/back branch ratio of less than 1 (1.45 ± 0.33 for control, 0.34 ± 0.10 for anti-DCC; $p = 0.01$; Fig. 5 F). Thus, while the anti-DCC treatment did not have opposite effects to those of netrin treatment (Figs. 1, 2), DCC receptor blockade significantly slowed the branching patterns of newly innervating RGC growth cones at their target.

Dynamic analysis of growth cones in stage 40 tadpoles revealed that anti-DCC treatment influenced branch addition and stabilization. Growth cones exposed to anti-DCC added significantly fewer branches throughout the 24 hr observation period (2hr intervals: 3.13 ± 0.33 added branches for control , 2.04 ± 0.25 for anti-DCC, p = 0.018; 6–24 hr interval: 10.50 ± 1.22 added branches for control, 5.75 ± 1.72 for anti-DCC; $p = 0.03$; Fig. 5 G) and also stabilized fewer branches during the first 6 hours after treatment (total stable branches: 6.13 ± 0.41 for control, 4.31 ± 0.35 for anti-DCC; $p = 0.002$; Fig. 5 H). Therefore, anti-DCC treatment exerted a significant effect on the dynamic growth of simple RGC axons in stage 40 tadpoles as they innervate the optic tectum, preventing overall growth. Dynamic analysis also revealed that, of the few forward branches that axons added after anti-DCC treatment, only a small proportion of those branches remained stable during each 2 hr observation interval (Fig. 5 I). Collectively, these results suggest that DCC signaling may be involved, at least in part, in the response of newly targeted RGC axons in stage 40 tadpoles to exogenous netrin-1 treatment we observed, but that mechanistically the signaling pathways involved in transducing responses to netrin may be complex.

Our results showed that netrin-1 treatment influenced the branching of RGC axon growth cones at their target in stage 40 tadpoles, but had no effect on newly targeted RGC axon growth cones at stage 45 (Fig. 4). To further examine the possibility that the age-dependent response by RGC axon growth cones involves DCC signaling, we also examined branching patterns of newly targeted RGC growth cones in stage 45 tadpoles after acute anti-DCC treatment. Treatment with anti-DCC had no effect on any of the branching parameters measured on stage 45 growth cones (data not shown), indicating that in contrast to stage 40, growth cone containing RGC axons at this developmental stage are unresponsive to both exogenous and endogenous netrin signaling.

RGC axonal growth cone migration in response to netrin-1 treatment in *vitro*

To further explore the mechanisms by which netrin influences branch initiation, we examined the acute response of RGC axon growth cones to netrin in a culture environment devoid of the target. This allowed us to determine if netrin treatment alone was sufficient to halt forward migration and back branching, as observed *in vivo*. In these experiments, *Xenopus* eye explant cultures were prepared from stage 25 tadpoles, and grown for 24 hours *in vitro*. By 24 hours, at a stage equivalent to stage 39/40 in the living tadpole, the behavior of RGC axons was followed by DIC time-lapse imaging. To examine effects of netrin treatment, cultures were imaged every 30 seconds for five minutes to obtain a baseline of growth cone movement. Following this imaging period, netrin-1 was applied to the culture medium at three different concentrations (10 ng/ml, 100 ng/ml, or 300 ng/ml final concentration), and imaging was resumed and continued for a total of one hour (Fig. 6 A, B). This allowed for observation of growth cone behavior pre and post-treatment. For all parameters analyzed, treatment with netrin-1 at 10 ng/ml had no significant effect on growth cones (data not shown). In contrast, growth cones exposed to netrin-1 at 100 ng/ml and 300 ng/ml responded in a dose-dependent manner. The forward growth of each axon was measured and the change in length from one time-point to the next was calculated to determine if growth cones halted their forward growth in the presence of netrin-1 (Fig. 6 C). Five time-points were used for analysis of changes over time (time 0; normalized for pretreatment behavior, and 2, 5, 10, 20 and 50 minutes following treatment). Data are presented as the relative change in axon length from each observation time-point to the end of the observation period. Application of netrin-1 at both concentrations examined (100 ng/ml and 300 ng/ml) significantly increased forward growth (0 – 50 min; 106.3 ± 6.23% for controls, 130.2 ± 5.37% for 100 ng/ml netrin; $p = 0.008$; 155.7 ± 12.64% for 300 ng/ml netrin vs control; $p = 0.003$, Fig. 6 C). This is in contrast to the effects of netrin *in vivo* for recently targeted growth cones at stage 40 (Fig. 1 C, D). Over the one-hour observation

period, control RGC axon growth cones in culture did not significantly increase their length from their starting point (Controls: 99.63 ± 2.79% increase in length from 0–2 min, 106.3 ± 6.23% from 0–50 min; $p = 0.34$). In contrast, netrin-1 treatment significantly increased forward growth at the two concentrations examined (100 ng/ml Netrin: 105.1 ± 2.46% from 0–2 min, 130.2 ± 5.37% from 0 to 50 min; p = 0.0003; 300 ng/ml Netrin 104.8 ± 2.75% for from 0–2 min, 155.7 ± 12.64% from 0 to 50 min; p = 0.0006). Thus, in contrast to its effects *in vivo*, acute netrin-1 treatment induced forward growth of RGC axon growth cones *in vitro*.

Netrin significantly impacts the morphology of the RGC axon growth cones in culture

In vivo observations of fluorescently labeled RGCs have shown that growth cones change their morphology as they navigate, becoming more complex at directional choice points and during targeting (Holt, 1989). To determine whether growth cone complexity is also influenced by netrin in the absence of a target, we examined the lamellipodial area of the growth cone, as well as the expanse of the growth cone filopodia in our time-lapse imaged cultures (see Fig. 7 A for an example of these measured areas). This allowed us to closely follow changes in growth cone morphology following netrin-1 treatment with fine temporal and spatial resolution. In the presence of 300 ng/ml netrin-1, growth cones decreased the area of the growth cone within 5–10 minutes of treatment (Change in growth cone area from 0–5 min: 0.65 ± 1.07 μm^2 for controls, -2.21 ± 0.92 μm^2 for 300 ng/ml netrin; $p = 0.06$), and this decrease persisted over the remainder of the observation period (Change in growth cone area from 0–50 min: 2.14 ± 1.52 μm^2 for controls, -3.01 ± 1.21 μm^2 for 300 ng/ml netrin; $p = 0.01$, Fig. 7 B, C). Similarly, cultures treated with netrin-1 at 100 ng/ml showed a significant decrease in lamellipodial growth cone area from controls 50 minutes after treatment (2.14 ± 1.52 μm^2 for controls, −2.29 ± 1.48 μm^2 for 100 ng/ml netrin; $p = 0.05$, Fig. 7 C). The expanse of the growth cone filopodia was also significantly decreased 50 minutes post-treatment at the two concentrations of netrin-1 used when compared to controls (Change in area encompasing growth cone processes from 0–50 min: 65.10 ± 38.78 μm^2 for control, −26.54 ± 21.01 μm^2 for 100 ng/ml netrin ; $p = 0.05$, Change in expanse of growth cone from 0–50 min: −55.15 ± 22.03 μm^2 for 300 ng/ml netrin from 0–50 min, compared to control from 0–50 min, $p = 0.01$; Fig. 7 D). Analysis of cultures following fixation at the end of the imaging period allowed for the examination of netrin responses by a larger population of RGC growth cones for each experiment in addition to those followed by time-lapse imaging. The growth cone area (9.83 ± 1.30 μm^2 for controls, 5.58 ± 0.68 μm^2 for netrin 300; p = 0.003) and the area encompassing the growth cone processes (257.5 ± 32.93 μm^2 for controls, 121.4 ± 13.06 μm^2 for 300 ng/ml netrin; p = 0.0001) were significantly smaller in RGC axons exposed to netrin-1 for 50 minutes than controls (not shown graphically), consistent with our dynamic observations in time-lapsed axons (Fig. 7 C, D). Together, the decreased lamellipodial area and filopodial expanse of the growth cone indicates that growth cones rapidly respond to netrin by acquiring a less complex morphology, reminiscent of active axon pathfinding morphology. The acute effects of netrin on RGC growth cones in culture at the time they innervate the tectum therefore differ from the chronic effects of netrin on more immature RGC axons (de la Torre et al, 1997).

RGC growth cones extend back branches as they continue their forward advancement in the presence of netrin-1 *in vitro*

To determine whether netrin influences RGC axon branching *in vitro*, we counted the number of filopodial processes on the growth cone, as well as processes behind the growth cone, in RGC axons in culture followed by time-lapse imaging. Within an hour of treatment, RGC axons had significantly fewer filopodial processes at the growth cone in the presence of netrin when compared to controls (Change in filopodia number from 0–50 min: 2.00 ± 1.54 for controls, ▫ 4.23 ± 1.43 for 300 ng/ml netrin; $p = 0.008$, Fig. 8 A–C). Similarly, the

number of filopodial processes at the growth cone was significantly lower in the total population of axons exposed to netrin-1 than in controls (Total branch number: 9.44 ± 0.61 for control, n= 34; 7.70 ± 0.48 for 100 ng/ml netrin, n= 38; p = 0.03, 6.66 ± 0.41 for 300ng/ml netrin, n= 77; p = 0.0006 when compared to control, not shown graphically). In contrast to the netrin-elicited decrease in the number of processes at the growth cone end, netrin-1 increased the number of processes behind the growth cone when compared to controls (Change in back branch number from 0–20 min: -0.36 ± 1.02 for control, 3.23 ± 1.21 for 300ng/ml netrin; p = 0.04; Change in back branch number from 0–50 min: −0.18 ± 1.27 for control, 3.62 ± 1.48 for 300ng/ml netrin; p = 0.07, Fig. 8 A–B, D). Short, spike-like processes of less than 1.5 μm in length were also increased within 2 minutes of netrin treatment (Fig. 8 A–B, E). As also observed for the imaged axons, the number processes behind the growth cone was significantly higher in the entire population of axons analyzed in fixed cultures one hour after treatment (1.50 ± 0.36 for control, n = 34; 3.17 ± 0.58 for 300ng/ml netrin, n = 77; p = 0.02, not shown graphically). Thus, similar to its effects *in vivo*, netrin induced back branching of RGC axon growth cones *in vitro*.

In the presence of netrin-1, RGC growth cones increase their density of presynaptic specializations and downregulate DCC expression

Previous reports from our group and others have shown that DCC-mediated netrin signaling is involved in presynaptic differentiation *in vivo* (Colon-Ramos et al, 2007; Manitt et al, 2009). To determine if netrin influences presynaptic differentiation in the absence of target cells, retinal cultures exposed to netrin-1 for one hour were fixed and immunostained with antibodies to the presynaptic protein SNAP-25 or antibodies to DCC. Cultures were also stained with rhodamine labeled phalloidin to correlate the organization of the actin cytoskeleton with the distribution of presynaptic specializations or DCC receptor protein. To quantify SNAP-25 or DCC immunoreactivity at the axon terminal, we obtained a value of immunopositive pixel number per unit axon length. This analysis revealed that axons exposed to netrin-1 had a significantly higher density of SNAP-25 immunoreactivity at their terminals compared to controls (7.68 ± 0.76 pixels/μm for control, 11.01 ± 1.25 for 100 ng/ml netrin; p = 0.02. 17.93 ± 1.10 pixels/μm for 300 ng/ml netrin, compared to control; p = 0.001, Fig. 9 A, C). Thus netrin impacts presynaptic differentiation of young RGC axons in culture, similar to previous observations of its effects on more mature RGC axons *in vivo* (Manitt et al., 2009). Analysis of DCC expression with two antibodies directed to distinct domains of the receptor revealed that the density of DCC immunostaining was lower in the growth cone-containing RGC axons exposed to netrin-1 for one hour when compared to vehicle treated controls (14.11 ± 1.61 pixels/μm for control, 8.49 ± 1.10 pixels/μm for 100 ng/ml netrin; p = 0.01. 10.23 ± 0.76 for 300 ng/ml netrin, compared to control; p = 0.02, Fig. 9 B, D). Together, these studies indicate that RGC axons respond to netrin by increasing presynaptic differentiation at their axon terminal, while also downregulating DCC protein levels, perhaps through signaling feedback mechanisms.

Discussion

To date, the responses of growth cones undergoing targeting events have been largely investigated in culture preparations, in part due to the difficulty of observing growth cones undergoing target innervation *in vivo*. Findings presented here describe a detailed time-lapse analysis of the branching patterns of single *Xenopus* RGC growth cones in living animals as they initiate branching soon after target innervation. By imaging individual RGC axons expressing fluorescent proteins, we show that following target entrance, RGC axons continued to advance within the target and added branches along the newly extended portion of the axon. Moreover, RGC axons simultaneously eliminated processes below the initial position of their growth cone during this period of growth cone advancement into the target

(from 0–6 hours). Later in the observation period, however, RGC axon growth cones increased their number of back branches as they coordinately halted their forward advancement into the target. Thus, as RGC axons enter their target they continue to advance and extend forward branches, possibly as an exploratory search for their correct topographical position. Upon locating their correct position within the target, axons then begin an active process of arborization through the addition and stabilization of collateral branches along the extent of the arbor, similar to the interstitial branching of RGC axons targeting in chick and rodent optic tectum (McLaughlin and O'Leary, 2005).

Netrin-1 impacts branch initiation in newly targeted RGC axons in the brain

By imaging recently targeted RGC axon growth cones in stage 40 tadpoles right before they begin to arborize, our studies demonstrate that acute netrin-1 treatment impacts early axon arbor differentiation by altering branching responses at the target. Dynamic *in vivo* imaging revealed that RGC axon growth cones halted their forward migration in the optic tectum upon an acute increase in netrin levels and displayed a specific increase in back branching within two to four hours after treatment. This early response of RGC axon growth cones to changes in netrin tectal levels significantly interfered with the arborization of RGC axons by 24 hours after treatment. The dynamic responses of RGC growth cones to netrin treatment suggest that endogenous netrin may serve early as a repulsive cue for newly targeted RGC axons that influences the onset of arbor maturation, therefore influencing the growth cone's decision of where to terminate. Indeed, *in vitro* responses of RGC axons to netrin at the stage that they exit the optic tract suggested that netrin may act as a repellant for young RGC axons as they innervate their target optic tectum (Shewan et al 2002). Evidence from culture studies investigating the response of RGC axons to Sema3A indicates that repulsive guidance cues can influence the initiation of branching following growth cone collapse (Campbell et al., 2001). *In vivo* imaging studies demonstrating a role for Slit-1 during the development of zebrafish retinotectal projections further support the idea that repulsive molecules can influence the time course of RGC arbor maturation at the target (Campbell et al., 2007).

The expression patterns of netrin in the developing optic tectum are consistent with a potential repulsive role for netrin on newly targeted RGC axons. Netrin mRNA is expressed in the *Xenopus* optic tectum at the developmental stages when presynaptic RGC axons first contact their target, caudally to the termination zone of RGC axons in the optic tectum of young tadpoles (Shewan et al, 2002; S. Marshak and S.C.C., unpublished results). Thus, RGC axon arbors can encounter netrin as they innervate their target and at the appropriate stage of development to begin to branch. Graded expression of netrin protein within the target optic tectum may explain, at least in part, the differential response of newly targeted RGC axons as they first innervate their target and of RGC axons that actively branch in the more mature tectal neuropil. Gradients of both repulsive and attractive axon guidance cues have been demonstrated to differentially guide axon pathfinding and targeting in the developing visual system (Frisen et al., 1998; Lyckman et al., 2001; Mann et al., 2002; McLaughlin and O'Leary, 2005; O'Leary and McLaughlin, 2005) , and graded distribution of netrin protein has also been demonstrated to guide axons in the spinal cord (Kennedy et al., 2006). Although netrin immunoreactivity can be detected in the optic tectum of both stage 40 and stage 45 tadpoles at the developmental stages when RGC axons reach the target and actively branch (Manitt et al., 2009, and C.M. and S.C.C., unpublished results), proof of netrin gradients in the *Xenopus* optic tectum remains elusive as reagents with enough sensitivity to unequivocally reveal such protein gradients are unavailable.

The age and maturation state of the RGC axon influence the axon's response to netrin

Our studies show that RGC axons exhibit an age- and maturation-dependent response to netrin and pertubations in DCC-mediated signaling *in vivo*. Specifically, growth cones in stage 45 tadpoles treated with netrin-1 did not halt their forward migration or show continued back branching as did growth cones in stage 40 netrin-treated tadpoles. Blocking DCC significantly impacted the forward and back branching patterns of growth cones at stage 40 but had no effect on growth cones at stage 45. In addition to an age-dependent branching response to netrin, a maturation-dependent response was observed when comparing simple, growth cone containing RGC axons to more differentiated RGC axons in tadpoles at the same stage (either stage 40 or 45). In stage 40 tadpoles, growth cones showed decreased branching, while more differentiated axon arbors did not respond to the netrin treatment. Conversely, in stage 45 tadpoles, simple growth cones were unaffected by netrin treatment while more branched axons responded with a robust increase in branch number by 24 hours. It is possible that this maturation-dependent branching response is due to intrinsic differences in the early, growth cone-containing axons versus more differentiated and branched axons, which reflect the differential wiring tasks being undertaken by the axon while it assumes these two different morphologies. These changes could be due to axons encountering different levels of endogenous netrin protein as they branch and advance within the tectal neuropil (as discussed above), and/or to differential activation of intracellular signaling pathways that may alter responsiveness to the same cue as axons change morphologically and as the extracellular environment changes as the brain matures (Ming et al., 1997; Shewan et al., 2002; Piper et al., 2005).

Changes in netrin receptor expression at the axon terminal may also underlie the differential age and maturation dependent response of RGC axons to netrin we observed. Immunostaining of RGC growth cones exposed to netrin-1 in culture showed that netrin influences the levels of DCC protein along the axon terminal (Fig. 9 B, D), supporting the existence of feedback mechanisms. Similar findings have been reported for cultured embryonic rat cortical neurons, which down regulate DCC after netrin application (Kim et al., 2005). Changes in DCC receptor expression may occur as part of an adaptation or desensitization response to excess netrin signaling that may serve to readjust the sensitivity to external molecular cues, similar to responses observed in migrating cells that undergo chemotaxis (Macnab and Koshland, 1972; Zigmond, 1977; Devreotes and Zigmond, 1988; Eisenbach, 1996; King and Insall, 2009). Indeed, *Xenopus* spinal and RGC growth cones in culture exhibit similar changes in responsiveness to molecular cues depending on the background concentration of that cue (Ming et al., 2002; Piper et al., 2005), a process that may involve rapid changes in receptor expression and/or desensitization.

In addition to rapid changes in DCC receptor expression and/or function in response to changes in netrin levels or signaling, intrinsic regulation of DCC or netrin expression may account for the developmental differences in effects we observed. Indeed, quantitative PCR studies showed that DCC and netrin-1 mRNA levels are dynamically regulated in the developing tadpole visual system (N.J.S. and S.C-C., data not shown). The observation that retinal DCC mRNA levels increase by 2.5 fold from stage 40 to stage 45 supports the notion that DCC expression is dynamically regulated in RGCs during active retinotectal targeting and axon branching. Thus age- and maturation-dependent changes in DCC receptor expression and function at the growth cone may underlie the differential responses of RGC axons to netrin as they mature.

Differential effects of DCC signaling on newly targeted RGC axons

Our data demonstrate that blocking DCC function affected growth cone advancement and back branching *in vivo,* preventing overall growth. RGC axon growth cones of stage 40

tadpoles exposed to anti-DCC function blocking antibodies significantly slowed their growth and branching, an effect that is similar to that of anti-DCC treatment on more elaborate RGC axons of stage 45 tadpoles (Manitt et al., 2009). Acute treatment with anti-DCC also prevented normal growth cone advancement within the target. The finding that anti-DCC did not exert inverse effects to those of excess netrin-1 treatment on growth cones of stage 40 tadpoles suggests that regulated changes in the level of netrin-1 signaling may modulate its function between a factor that initiates branching and one that promotes axon outgrowth. This possibility is supported by studies showing that effects of netrin-1 are tightly regulated by dosage, as doses above or below a threshold netrin level can inhibit axon outgrowth of spinal neurons (Serafini et al., 1994). It is also possible that the differential effects of netrin and anti-DCC treatments may be due to activation of netrin receptors other than DCC within the retinotectal circuit. An additional, non-exclusive possibility is that DCC may interact with other co-factors or co-receptors that influence the targeting and branching of RGC axons. Evidence demonstrating that DCC can interact with Robo (Stein and Tessier-Lavigne, 2001), UNC5 (Hong et al., 1999), A2b (Corset et al., 2000), DSCAM (Liu et al., 2008; Ly et al., 2008), heparin sulfate proteoglycans (Matsumoto et al., 2007), and metalloproteinases (Galko and Tessier-Lavigne, 2000a), supports the potential for a modulatory control of DCC-mediated netrin signaling as axon branching and differentiation proceeds.

Differential responses of RGC axon growth cones to netrin in the absence of a target

Our *in vivo* and *in vitro* findings suggest that growth cone advancement and axon back branching are mechanistically distinct processes. While recombinant netrin-1 induced back branching responses both *in vitro* and *in vivo*, the ability of netrin to inhibit growth cone advancement within the target *in vivo* was not recapitulated in culture. In fact, growth cones exposed to netrin-1 *in vitro* increased their rate of outgrowth while simultaneously adding back branches along the axon. Thus, netrin-1 signaling alone appears sufficient to modulate back branching, but additional cues provided by the surrounding target tissue may be needed for netrin-1 to halt forward advancement and induce branching. Consistent with this, calcium/calmodulin-dependent signaling has been shown to influence cortical axon elongation in culture but not in an *in vivo* context (Ageta-Ishihara et al., 2009). This supports the idea that growth cones integrate multiple cues in their local environment to modulate axon elongation and branching, by differentially influencing cytoskeletal remodeling. Additional cues shown to influence RGC axon entrance into the target *in vivo* include fibroblast growth factor (FGF) and its signaling molecules (McFarlane et al., 1995; McFarlane et al., 1996; Atkinson-Leadbeater et al., 2010), heparin sulfate proteoglycans (Walz et al., 1997; Irie et al., 2002), Robo receptors (Plachez et al., 2008; Hocking et al., 2010), and the matrix metalloproteinase ADAM10 (Chen et al., 2007). It is therefore possible that complex molecular interactions that normally occur in the intact target are necessary for netrin-1 to differentially activate specific intracellular signaling cascades and function as a stop signal for innervating RGC axons. The *in vivo* regulatory mechanisms by which netrin influences newly targeted RGC axons, and the interactions between its co-factors and co-receptors in this process are important new possibilities that remain open to investigation.

Acknowledgments

We thank Dr. Jorge Busciglio for access to his culture imaging facility, and Dr. Karina Cramer, Dr. Marcelo Wood and members of our laboratory for helpful comments on our manuscript. Supported by the National Eye Institute (EY011912).

References

Ageta-Ishihara N, Takemoto-Kimura S, Nonaka M, Adachi-Morishima A, Suzuki K, Kamijo S, Fujii H, Mano T, Blaeser F, Chatila TA, Mizuno H, Hirano T, Tagawa Y, Okuno H, Bito H. Control of cortical axon elongation by a GABA-driven Ca2+/calmodulin-dependent protein kinase cascade. J Neurosci. 2009; 29:13720–13729. [PubMed: 19864584]

Alsina B, Vu T, Cohen-Cory S. Visualizing synapse formation in arborizing optic axons in vivo: dynamics and modulation by BDNF. Nat Neurosci. 2001; 4:1093–1101. [PubMed: 11593233]

Atkinson-Leadbeater K, Bertolesi GE, Hehr CL, Webber CA, Cechmanek PB, McFarlane S. Dynamic expression of axon guidance cues required for optic tract development is controlled by fibroblast growth factor signaling. J Neurosci. 2010; 30:685–693. [PubMed: 20071533]

Brose K, Tessier-Lavigne M. Slit proteins: key regulators of axon guidance, axonal branching, and cell migration. Curr Opin Neurobiol. 2000; 10:95–102. [PubMed: 10679444]

Brose K, Bland KS, Wang KH, Arnott D, Henzel W, Goodman CS, Tessier-Lavigne M, Kidd T. Slit proteins bind Robo receptors and have an evolutionarily conserved role in repulsive axon guidance. Cell. 1999; 96:795–806. [PubMed: 10102268]

Campbell DS, Regan AG, Lopez JS, Tannahill D, Harris WA, Holt CE. Semaphorin 3A elicits stage-dependent collapse, turning, and branching in Xenopus retinal growth cones. J Neurosci. 2001; 21:8538–8547. [PubMed: 11606642]

Campbell DS, Stringham SA, Timm A, Xiao T, Law MY, Baier H, Nonet ML, Chien CB. Slit1a inhibits retinal ganglion cell arborization and synaptogenesis via Robo2-dependent and -independent pathways. Neuron. 2007; 55:231–245. [PubMed: 17640525]

Chen YY, Hehr CL, Atkinson-Leadbeater K, Hocking JC, McFarlane S. Targeting of retinal axons requires the metalloproteinase ADAM10. J Neurosci. 2007; 27:8448–8456. [PubMed: 17670992]

Colon-Ramos DA, Margeta MA, Shen K. Glia promote local synaptogenesis through UNC-6 (netrin) signaling in C. elegans. Science. 2007; 318:103–106. [PubMed: 17916735]

Corset V, Nguyen-Ba-Charvet KT, Forcet C, Moyse E, Chedotal A, Mehlen P. Netrin-1-mediated axon outgrowth and cAMP production requires interaction with adenosine A2b receptor. Nature. 2000; 407:747–750. [PubMed: 11048721]

Davenport RW, Thies E, Nelson PG. Cellular localization of guidance cues in the establishment of retinotectal topography. J Neurosci. 1996; 16:2074–2085. [PubMed: 8604052]

Davenport RW, Thies E, Cohen ML. Neuronal growth cone collapse triggers lateral extensions along trailing axons. Nat Neurosci. 1999; 2:254–259. [PubMed: 10195218]

de la Torre JR, Hopker VH, Ming GL, Poo MM, Tessier-Lavigne M, Hemmati-Brivanlou A, Holt CE. Turning of retinal growth cones in a netrin-1 gradient mediated by the netrin receptor DCC. Neuron. 1997; 19:1211–1224. [PubMed: 9427245]

Deiner MS, Kennedy TE, Fazeli A, Serafini T, Tessier-Lavigne M, Sretavan DW. Netrin-1 and DCC mediate axon guidance locally at the optic disc: loss of function leads to optic nerve hypoplasia. Neuron. 1997; 19:575–589. [PubMed: 9331350]

Devreotes PN, Zigmond SH. Chemotaxis in eukaryotic cells: a focus on leukocytes and Dictyostelium. Annu Rev Cell Biol. 1988; 4:649–686. [PubMed: 2848555]

Eisenbach M. Control of bacterial chemotaxis. Mol Microbiol. 1996; 20:903–910. [PubMed: 8809743]

Frisen J, Yates PA, McLaughlin T, Friedman GC, O'Leary DD, Barbacid M. Ephrin-A5 (AL-1/RAGS) is essential for proper retinal axon guidance and topographic mapping in the mammalian visual system. Neuron. 1998; 20:235–243. [PubMed: 9491985]

Galko MJ, Tessier-Lavigne M. Function of an axonal chemoattractant modulated by metalloprotease activity. Science. 2000a; 289:1365–1367. [PubMed: 10958786]

Harris WA, Holt CE, Bonhoeffer F. Retinal axons with and without their somata, growing to and arborizing in the tectum of Xenopus embryos: a time-lapse video study of single fibres in vivo. Development. 1987; 101:123–133. [PubMed: 3449363]

Hocking JC, Hehr CL, Bertolesi GE, Wu JY, McFarlane S. Distinct roles for Robo2 in the regulation of axon and dendrite growth by retinal ganglion cells. Mech Dev. 2010; 127:36–48. [PubMed: 19961927]

Holt CE. A single-cell analysis of early retinal ganglion cell differentiation in Xenopus: from soma to axon tip. J Neurosci. 1989; 9:3123–3145. [PubMed: 2795157]

Hong K, Hinck L, Nishiyama M, Poo MM, Tessier-Lavigne M, Stein E. A ligand-gated association between cytoplasmic domains of UNC5 and DCC family receptors converts netrin-induced growth cone attraction to repulsion. Cell. 1999; 97:927–941. [PubMed: 10399920]

Hopker VH, Shewan D, Tessier-Lavigne M, Poo M, Holt C. Growth-cone attraction to netrin-1 is converted to repulsion by laminin-1. Nature. 1999; 401:69–73. [PubMed: 10485706]

Hu B, Nikolakopoulou AM, Cohen-Cory S. BDNF stabilizes synapses and maintains the structural complexity of optic axons in vivo. Development. 2005; 132:4285–4298. [PubMed: 16141221]

Irie A, Yates EA, Turnbull JE, Holt CE. Specific heparan sulfate structures involved in retinal axon targeting. Development. 2002; 129:61–70. [PubMed: 11782401]

Kennedy TE, Wang H, Marshall W, Tessier-Lavigne M. Axon guidance by diffusible chemoattractants: a gradient of netrin protein in the developing spinal cord. J Neurosci. 2006; 23:8866–8874. [PubMed: 16928876]

Kim TH, Lee HK, Seo IA, Bae HR, Suh DJ, Wu J, Rao Y, Hwang KG, Park HT. Netrin induces down-regulation of its receptor, Deleted in Colorectal Cancer, through the ubiquitin-proteasome pathway in the embryonic cortical neuron. J Neurochem. 2005; 95:1–8. [PubMed: 16181408]

King JS, Insall RH. Chemotaxis: finding the way forward with Dictyostelium. Trends Cell Biol. 2009; 19:523–530. [PubMed: 19733079]

Liu G, Li W, Wang L, Kar A, K-L G, Rao Y, Wu J. DSCAM functions as a netrin receptor in commissural axon pathfinding. Proc Natl Acad Sci USA. 2008; 106:2951–2956. [PubMed: 19196994]

Ly A, Nikolaev A, Suresh G, Zheng Y, Tessier-Lavigne M, Stein E. DSCAM is a netrin receptor that collaborates with DCC in mediating turning responses to netrin-1. Cell. 2008; 133:1241–1254. [PubMed: 18585357]

Lyckman AW, Jhaveri S, Feldheim DA, Vanderhaeghen P, Flanagan JG, Sur M. Enhanced plasticity of retinothalamic projections in an ephrin-A2/A5 double mutant. J Neurosci. 2001; 21:7684–7690. [PubMed: 11567058]

Macnab RM, Koshland DE Jr. The gradient-sensing mechanism in bacterial chemotaxis. Proc Natl Acad Sci U S A. 1972; 69:2509–2512. [PubMed: 4560688]

Manitt C, Nikolakopoulou AM, Almario DR, Nguyen SA, Cohen-Cory S. Netrin participates in the development of retinotectal synaptic connectivity by modulating axon arborization and synapse formation in the developing brain. J Neurosci. 2009; 29:11065–11077. [PubMed: 19741113]

Mann F, Ray S, Harris W, Holt C. Topographic mapping in dorsoventral axis of the Xenopus retinotectal system depends on signaling through ephrin-B ligands. Neuron. 2002; 35:461–473. [PubMed: 12165469]

Marshak S, Nikolakopoulou AM, Dirks R, Martens GJ, Cohen-Cory S. Cell autonomous TrkB signaling in presynaptic retinal ganglion cells mediates axon arbor growth and synapse maturation during the establishment of retinotectal synaptic connectivity. J Neurosci. 2007; 27:2444–2456. [PubMed: 17344382]

Matsumoto Y, Irie F, Inatani M, Tessier-Lavigne M, Yamaguchi Y. Netrin-1/DCC signaling in commissural axon guidance requires cell-autonomous expression of heparan sulfate. J Neurosci. 2007; 27:4342–4350. [PubMed: 17442818]

McFarlane S, McNeill L, Holt CE. FGF signaling and target recognition in the developing Xenopus visual system. Neuron. 1995; 15:1017–1028. [PubMed: 7576646]

McFarlane S, Cornel E, Amaya E, Holt CE. Inhibition of FGF receptor activity in retinal ganglion cell axons causes errors in target recognition. Neuron. 1996; 17:245–254. [PubMed: 8780648]

McLaughlin T, O'Leary DD. Molecular gradients and development of retinotopic maps. Annu Rev Neurosci. 2005; 28:327–355. [PubMed: 16022599]

Ming GL, Song HJ, Berninger B, Holt CE, Tessier-Lavigne M, Poo MM. cAMP-dependent growth cone guidance by netrin-1. Neuron. 1997; 19:1225–1235. [PubMed: 9427246]

Ming GL, Wong ST, Henley J, Yuan XB, Song HJ, Spitzer NC, Poo MM. Adaptation in the chemotactic guidance of nerve growth cones. Nature. 2002; 417:411–418. [PubMed: 11986620]

Nieuwkoop, PD.; Faber, J. Normal Table of Xenopus laevis. The Netherlands: Elsevier North Holland; 1956.

O'Leary DD, McLaughlin T. Mechanisms of retinotopic map development: Ephs, ephrins, and spontaneous correlated retinal activity. Prog Brain Res. 2005; 147:43–65. [PubMed: 15581697]

Piper M, Salih S, Weinl C, Holt CE, Harris WA. Endocytosis-dependent desensitization and protein synthesis-dependent resensitization in retinal growth cone adaptation. Nat Neurosci. 2005; 8:179–186. [PubMed: 15643427]

Plachez C, Andrews W, Liapi A, Knoell B, Drescher U, Mankoo B, Zhe L, Mambetisaeva E, Annan A, Bannister L, Parnavelas JG, Richards LJ, Sundaresan V. Robos are required for the correct targeting of retinal ganglion cell axons in the visual pathway of the brain. Mol Cell Neurosci. 2008; 37:719–730. [PubMed: 18272390]

Serafini T, Kennedy TE, Galko MJ, Mirzayan C, Jessell TM, Tessier-Lavigne M. The netrins define a family of axon outgrowth-promoting proteins homologous to C. elegans UNC-6. Cell. 1994; 78:409–424. [PubMed: 8062384]

Shewan D, Dwivedy A, Anderson R, Holt CE. Age-related changes underlie switch in netrin-1 responsiveness as growth cones advance along visual pathway. Nat Neurosci. 2002; 5:955–962. [PubMed: 12352982]

Stein E, Tessier-Lavigne M. Hierarchical organization of guidance receptors: silencing of netrin attraction by slit through a Robo/DCC receptor complex. Science. 2001; 291:1928–1938. [PubMed: 11239147]

Walz A, McFarlane S, Brickman YG, Nurcombe V, Bartlett PF, Holt CE. Essential role of heparan sulfates in axon navigation and targeting in the developing visual system. Development. 1997; 124:2421–2430. [PubMed: 9199368]

Wang KH, Brose K, Arnott D, Kidd T, Goodman CS, Henzel W, Tessier-Lavigne M. Biochemical purification of a mammalian slit protein as a positive regulator of sensory axon elongation and branching. Cell. 1999; 96:771–784. [PubMed: 10102266]

Yates PA, Roskies AL, McLaughlin T, O'Leary DD. Topographic-specific axon branching controlled by ephrin-As is the critical event in retinotectal map development. J Neurosci. 2001; 21:8548–8563. [PubMed: 11606643]

Zigmond SH. Ability of polymorphonuclear leukocytes to orient in gradients of chemotactic factors. J Cell Biol. 1977; 75:606–616. [PubMed: 264125]

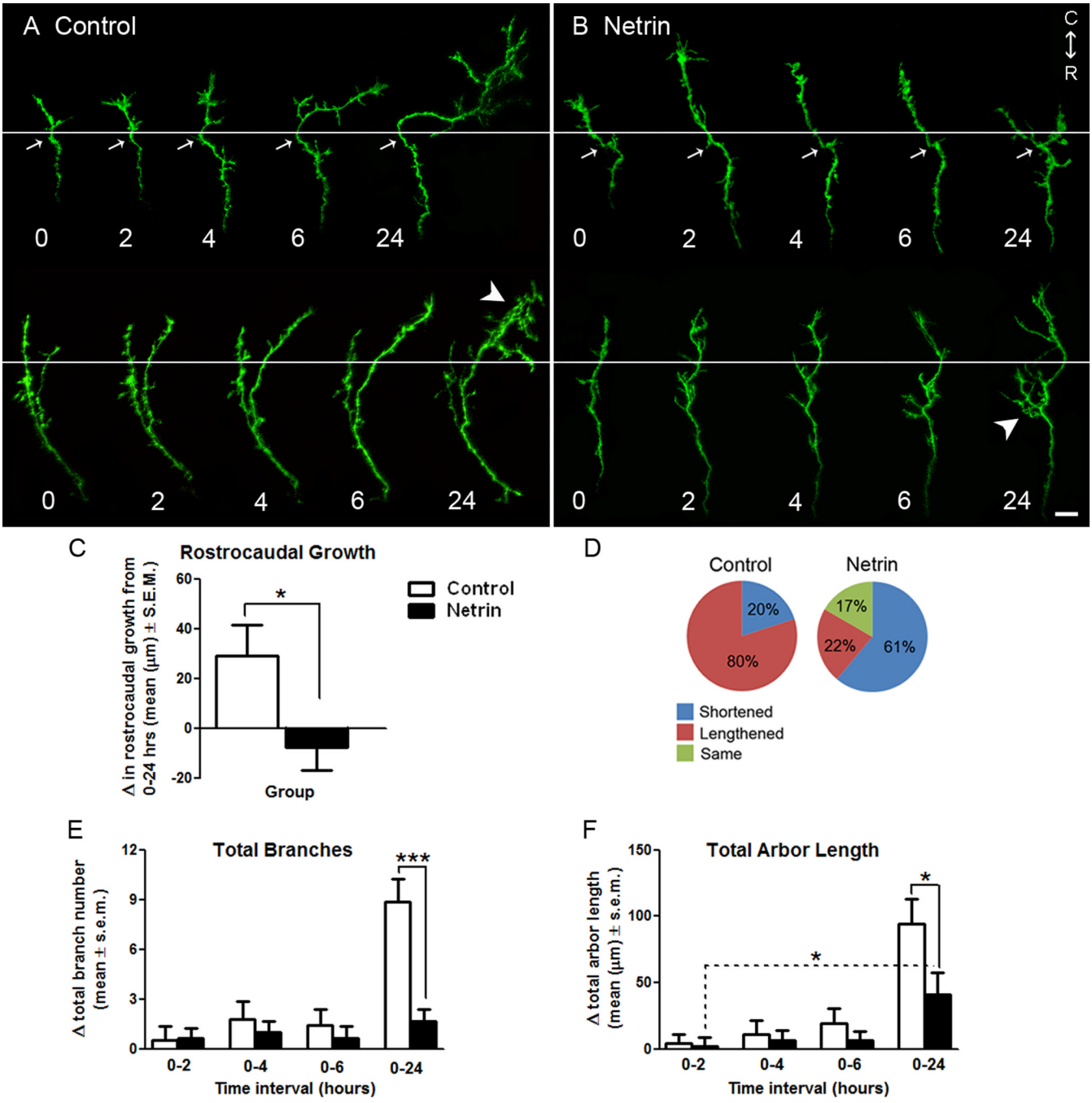

Figure 1. Netrin influences the forward advancement and morphology of RGC axon growth cones at their target

A, B) Representative reconstructions of control (**A**), and netrin-treated (**B**), RGC axon growth cones in stage 40 tadpoles expressing EYFP imaged by time-lapse confocal microscopy over 24 hours. White horizontal lines delineate the forward-back branching boundary used for quantification of axon growth (also see diagram in Fig. 2 A). White arrows indicate examples of intrinsic landmarks (bends in the axon) common to all time points that were used to align images. White arrowheads demarcate differences in the branching patterns of growth cones exposed to control vehicle solution or recombinant netrin (see Fig. 2). Illustrated portions of the axons lie completely within the optic tectum,

and rostral to caudal (R-C) orientation of the brain is indicated. Scale bar, 10 μm. **C, D)** A measure of rostro-caudal growth is provided by the change in length of axons exposed to control or netrin treatment over a 24 hour period (**C**), as well as the proportion of axons that lengthened, shortened or remained the same length throughout the observation period (**D**). Note that while the majority axons in control tadpoles lengthened, axons exposed to netrin-1 shortened over time or remained the same length. **E, F)** The effects of netrin-1 treatment on RGC axon growth cones of stage 40 tadpoles were further determined by quantifying the changes in total branch number (**E**), and total arbor length (**F**), at each time point relative to time 0. While changes in total branch number and length were similar for axons in control and netrin-treated tadpoles during the first six hours of imaging, a delayed effect of netrin is observed on branch number and length by 24 hours. Dotted lines indicate within group comparisons; solid lines represent between group comparisons. * signifies $p < 0.05$, *** $p < 0.0005$. Error bars indicate SEM.

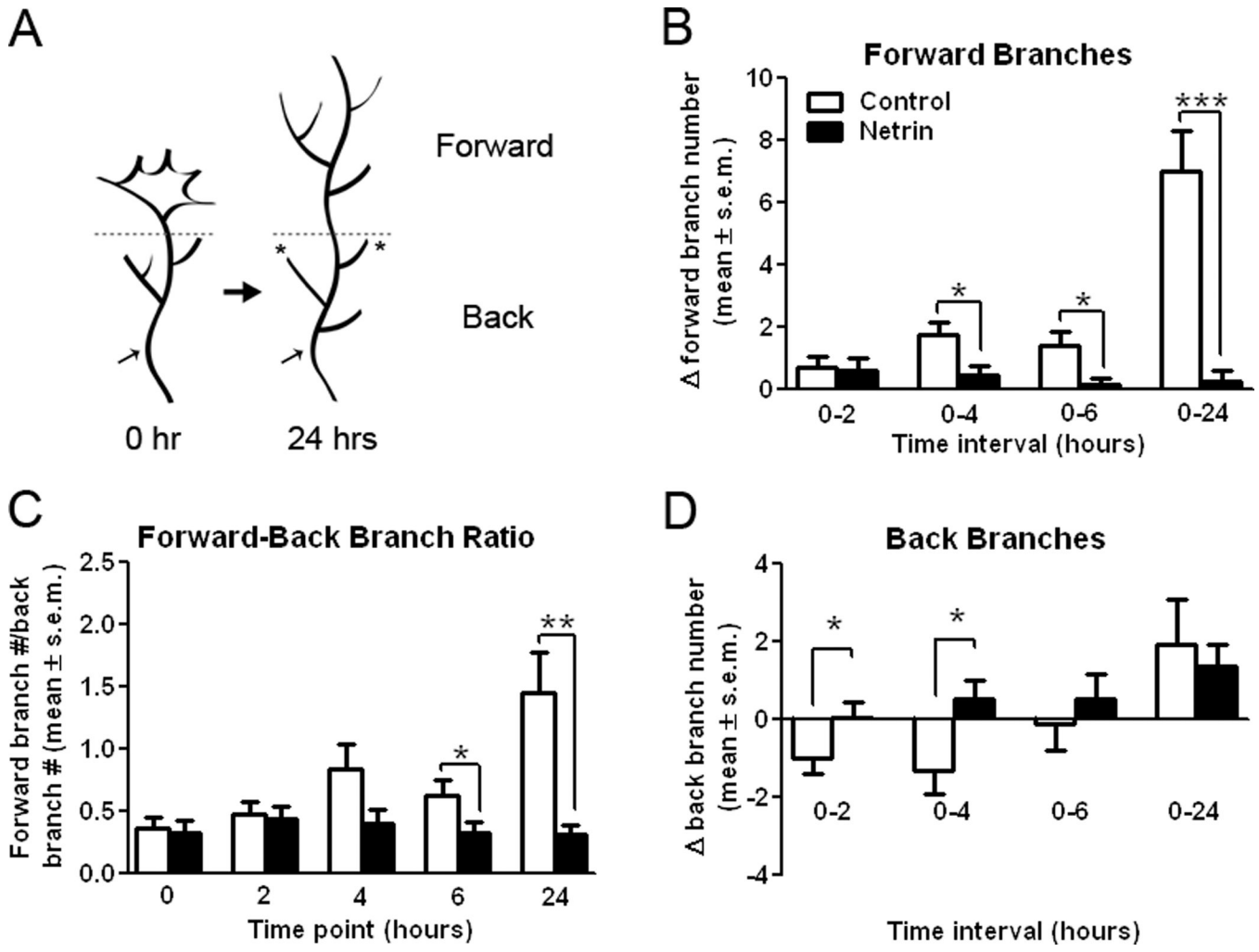

Figure 2. Netrin-1 differentially influences forward versus back branching of simple RGC axons in stage 40 tadpoles

A) Diagrammatic representation of the method used to differentiate forward versus back branching. A horizontal dotted line was used to delineate the forward-to-back branch boundary on RGC growth cones imaged over time. Asterisks are used to denote stable branches which persisted throughout the observation period; these stable branches, along with distinctive bends and swells in the axon (black arrows), were used as landmarks for image alignment along the forward-back branch boundary line. **B, D)** The difference in the number of total forward (**B**), or back (**D**), branches in RGC axons imaged over time was quantified for EYFP-expressing axons in control stage 40 tadpoles and in tadpoles injected with netrin-1 immediately after the initial imaging (time 0). Note the significant effect of netrin treatment on the number of both forward and back branches on RGC axon growth cones four hours after treatment. Netrin transiently and significantly increased the proportion of back branches between 0–4 hours relative to controls (**D**), but prevented the increase in forward branches observed in controls (**B**). **C)** A forward-to-back branch ratio provides an additional measure of axon growth. As RGC axon growth cones branched in the optic tectum, they extended a greater portion of forward than back branches, as indicated by a mean forward-to-back branch ratio greater than 1. A forward-to-back branch ratio of less than 1 as time proceeds is indicative of decreased forward growth relative to the degree of

back branching. Solid lines represent between-group comparisons. * $p < 0.05$; **$p < 0.005$, and *** $p < 0.0005$. Error bars indicate SEM.

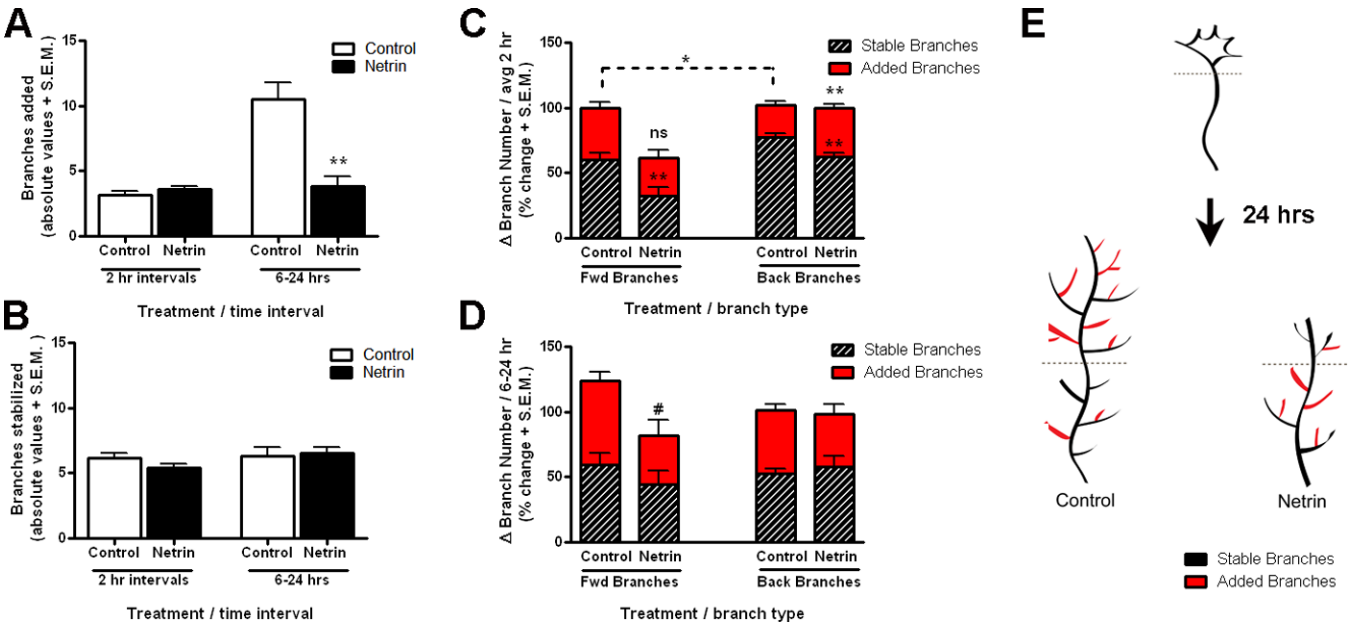

Figure 3. Netrin influences the dynamic branching behavior of recently targeted RGC axons

A–B) The dynamic behavior of recently targeted RGC axon growth cones in stage 40 tadpoles is illustrated by the quantification of total branch addition and branch stabilization for every two-hour interval during the first six hours after treatment (average 2 hr interval), and between 6 and 24 hours. **A)** Note that the number of new branches added was similar for newly targeted RGC axons exposed to netrin-1 as for controls during the first six hours after treatment but was significantly decreased later in the observation period. **B)** Analysis of stable branch number reveals that the number of stable branches was similar for control RGC axons and for those exposed to netrin-1 at all time intervals. **C, D)** The relationship between branch addition and stabilization of forward versus back branches was measured for each individual axon and is illustrated by the stacked bar graphs. **C)** In proportion, more new forward branches than back branches were added in control axons during every 2 hr observation interval, while a similar number of forward versus back branches were added in axons in netrin-treated tadpoles. Note that, in proportion, significantly more new back branches were added in axons exposed to netrin-1 than in controls. **D)** No significant difference in the proportion of added and stable forward versus back branches was observed between 6 and 24 hrs after initial imaging for controls or axons exposed to netrin-1. In *C, D*, stacked bars with a value above 100% represent intervals when more of the newly added branches were stabilized than eliminated. Conversely, stacked bars with a total value of less than 100% represent axons where in proportion more branches were eliminated than added at each corresponding time interval. # signifies $0.05 < p < 0.10$; *$p < 0.05$; **$p < 0.005$, and *** $p < 0.0005$, ns = non significant versus control. A dashed line represents comparisons within treatment group. Error bars indicate SEM. **E)** Diagrammatic representation of the differential branch addition and stabilization in differentiating RGC axon growth cones in control tadpoles versus tadpoles exposed to netrin 24 hours after treatment.

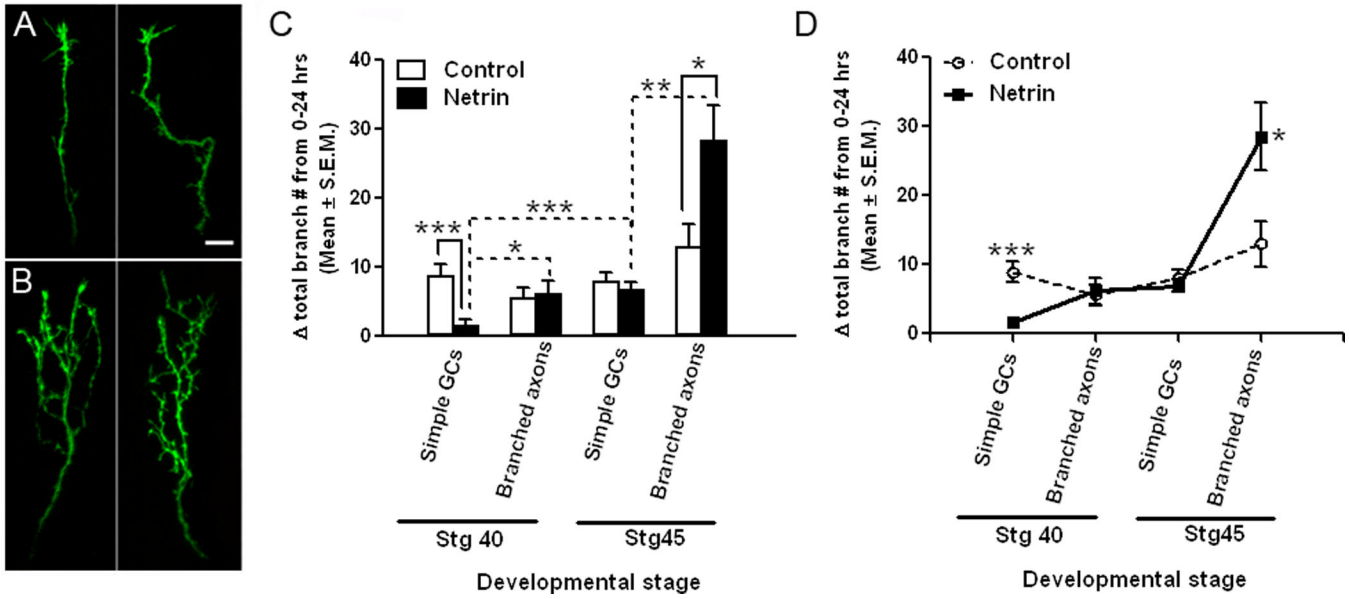

Figure 4. The age and morphological state of the RGC axon affect its branching response to netrin-1 *in vivo*

A, B) Representative images of two distinct RGC axon growth cones (**A**), and two branched RGC axons (**B**), in stage 40 tadpoles at time 0. RGC axon growth cones and branched axons of stage 45 tadpoles possessed morphologies similar those of stage 40 tadpoles (not shown). Scale bar, 10 μm. **C, D)** The difference in branching rates of RGC axon growth cones (Simple GCs) and branched arbors (Branched axons) of stage 40 versus stage 45 tadpoles in control-treated and netrin-treated tadpoles is shown graphically by the increase in total branch number over 24 hours. **C)** The increase in branch number (delta total branch number) over a 24 hour period is not significantly different for RGC axons in control tadpoles at the two developmental stages examined (stage 40 and stage 45), or for RGC axons with simpler or more complex arbors (simple growth cones or branched axons). Note the differential effect of netrin on simple growth cones of stage 40 tadpoles, and on branched RGC axons of stage 45 tadpoles, when compared to age- and morphology-matched controls. **D)** The difference in the branching rates of RGC axons exposed to netrin is better illustrated by the line graph of data shown in *C*. Data on branched RGC axons of stage 45 tadpoles is as published in Manitt et al, 2009. Dotted lines indicate within group comparisons; solid lines represent between group comparisons. * signifies $p < 0.05$; **$p < 0.005$, and *** $p < 0.0005$. Error bars indicate SEM.

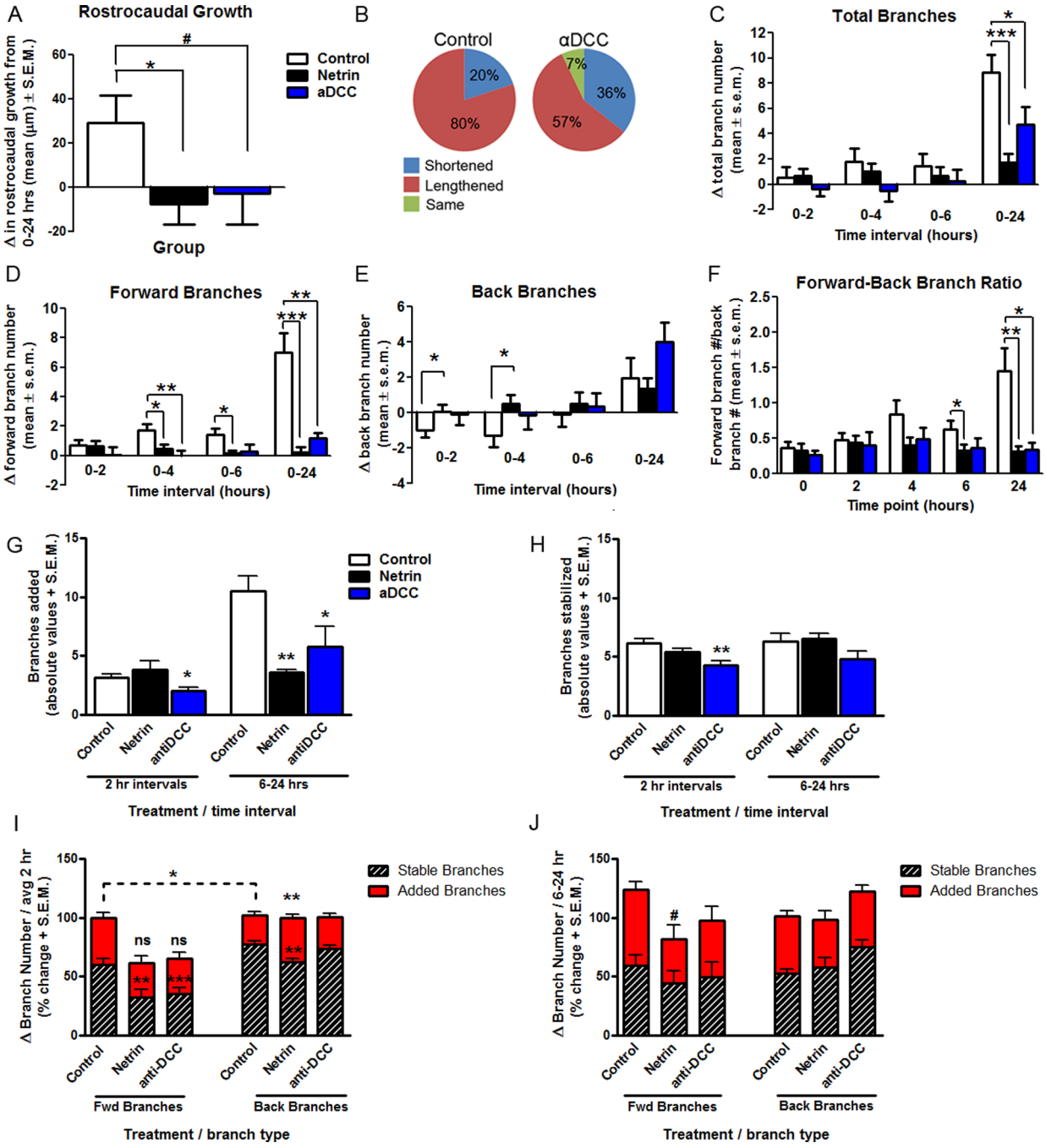

Figure 5. DCC receptor blockade interferes with RGC axon growth cone branching in stage 40 tadpoles

A, B) The effects of acute anti-DCC treatment on simple RGC axons of stage 40 tadpoles 24 hours after treatment on rostrocaudal growth is illustrated by the average change in axon length from its initial position at time 0 (*A*), and by the relative proportion of RGC axons that shortened, lengthened or remained the same length (*B*).**C–E)** The effects of DCC receptor blockade on the branching of RGC axon growth cones is shown by the quantification of the change in total branch number (*C*), and the change in forward (*D*) versus back (*E*), branches from the initial observation period to the next. Note that anti-DCC treatment interfered with axon branching when compared to controls (*D*), an effect that was

significant on forward branches (*D*), but not on back branches *(E)*. **F)** Axons exposed to anti-DCC treatment had a forward-back branch ratio that differed significantly from that of controls by 24 hours. **G-J)** The effects of anti-DCC treatment on branch dynamics of RGC growth cones is illustrated by the total number of branches added *(G)* and stabilized *(H),* and by the proportion of added and stable forward versus back branches *(I, J)* during every 2 hr observation interval and between 6 and 24 hours. Note that in contrast to control and netrin-1 treatment, anti-DCC treatment decreased both the addition and stabilization of branches. However in proportion, dynamic changes in branch addition of forward versus back branches were similar to control. *$p < 0.05$, **$p < 0.005$, and *** $p < 0.0005$. Error bars indicate SEM.

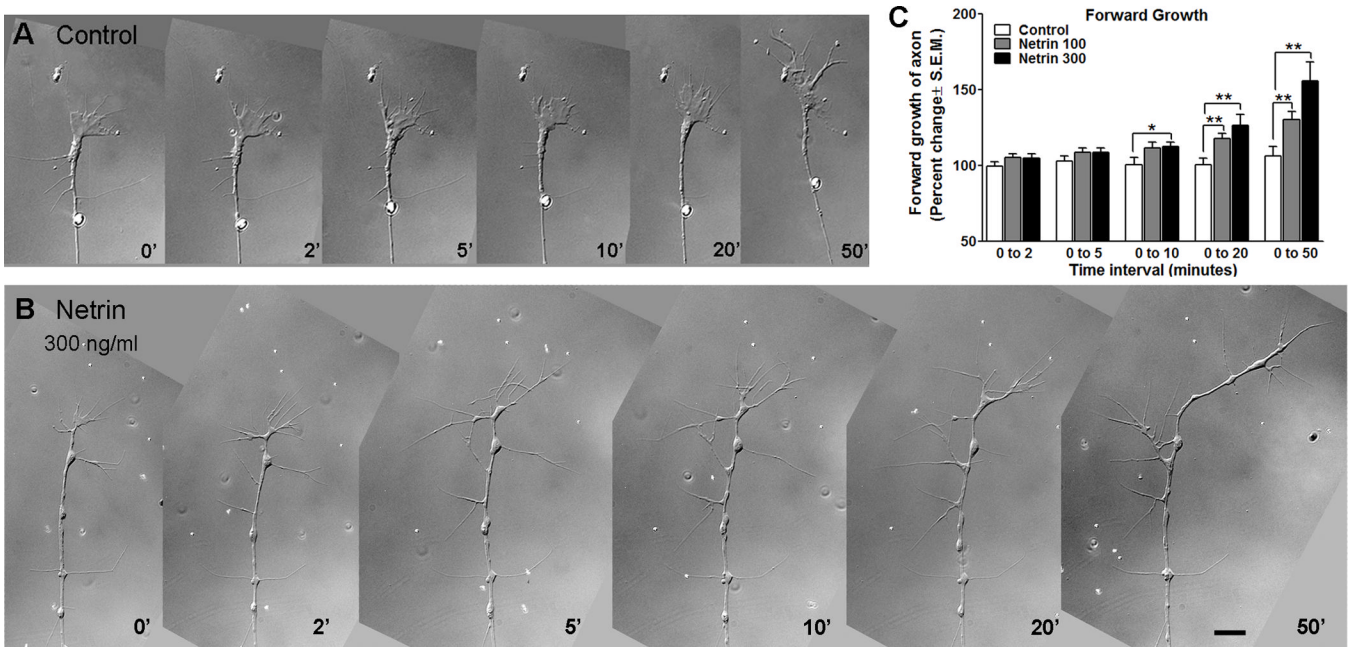

Figure 6. In culture, RGC axon growth cones respond to acute netrin treatment with increased forward growth

A, B) Time-lapse sequence of sample RGC axon growth cones imaged in culture under control conditions (*A*) and following acute exposure to netrin-1 (*B*). Scale bar, 10 μm. **C)** The increase in forward advancement of the growth cone from time 0 to subsequent observation intervals is shown by the relative increase in length for each individual axon (time 0 equals 100%). Note that treatment with netrin significantly increased the forward advancement of RGC growth cones in culture 10 minutes after treatment, in a dose-dependent manner.

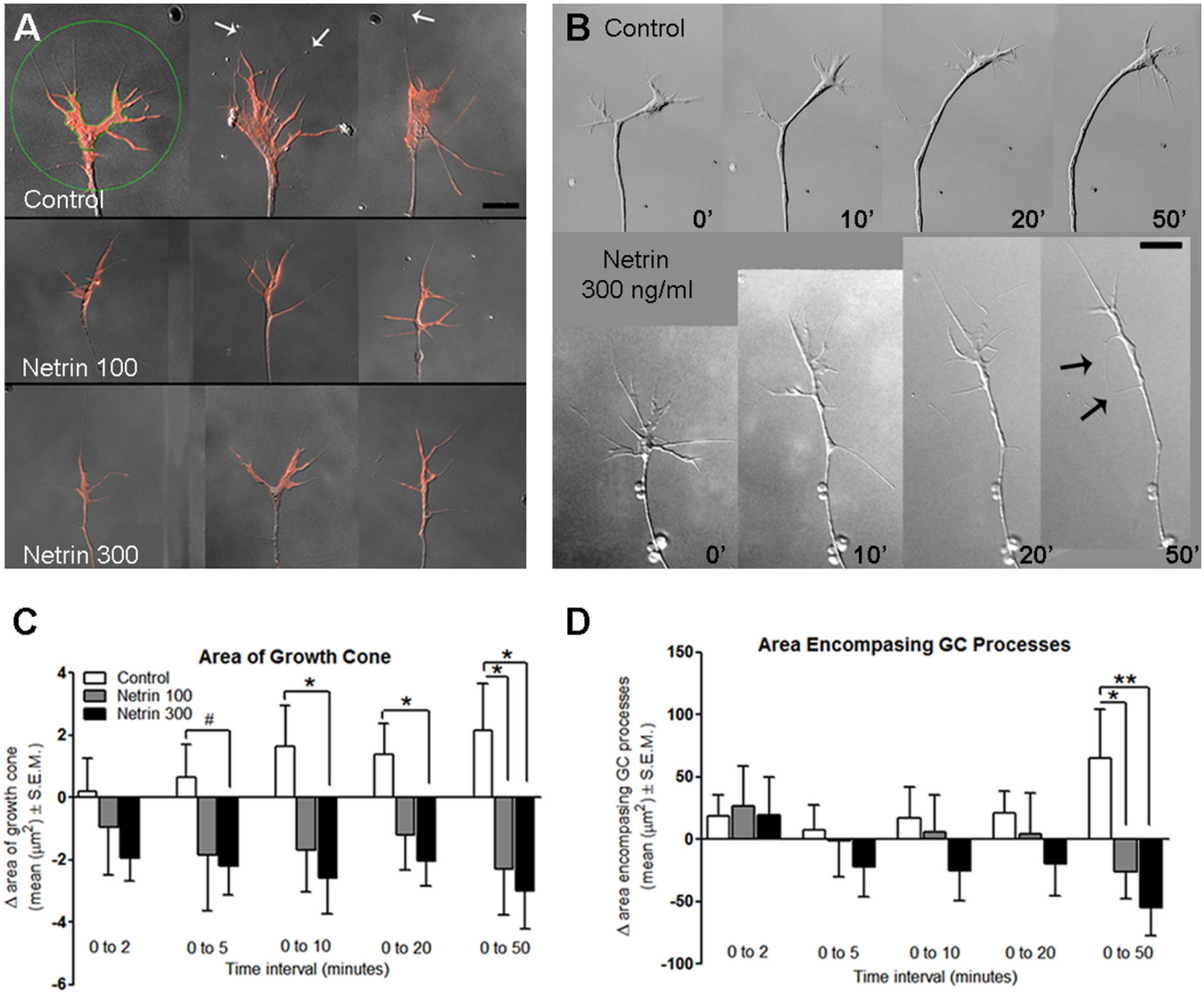

Figure 7. Dynamic growth cone changes in RGC axons in response to netrin treatment

A) Representative images from growth cones in culture fixed one hour post-treatment, stained with rhodamine phalloidin (red), serve to illustrate the changes in growth cone morphology in response to netrin treatment. The green circle and the green line around the lamellipodial perimeter in the first sample serve to illustrate the areas selected for measurement of lamellipodial area, and area encompassing the growth cone processes, respectively. White arrows indicate filopodial processes in growth cones. **B)** Dynamic changes in RGC axon growth cone morphology following netrin treatment are illustrated by this example (time 0). Black arrows point to processes newly extended by the growing axon (see also Fig 8). Scale bar for A and B, 10 μm. **E)** Measurements of the lamellipodial area of the growth cone show that within five minutes of netrin treatment the area of the growth cone decreases in size, a behavior that is different from controls. **F)** Measurement of the area encompassing the filopodial processes on the growth cone show that netrin treatment gradually decreased the radial spread of the growth cone processes, an effect that became significantly different from controls 50 minutes post-treatment. * $p < 0.05$; **$p < 0.005$. Error bars indicate SEM.

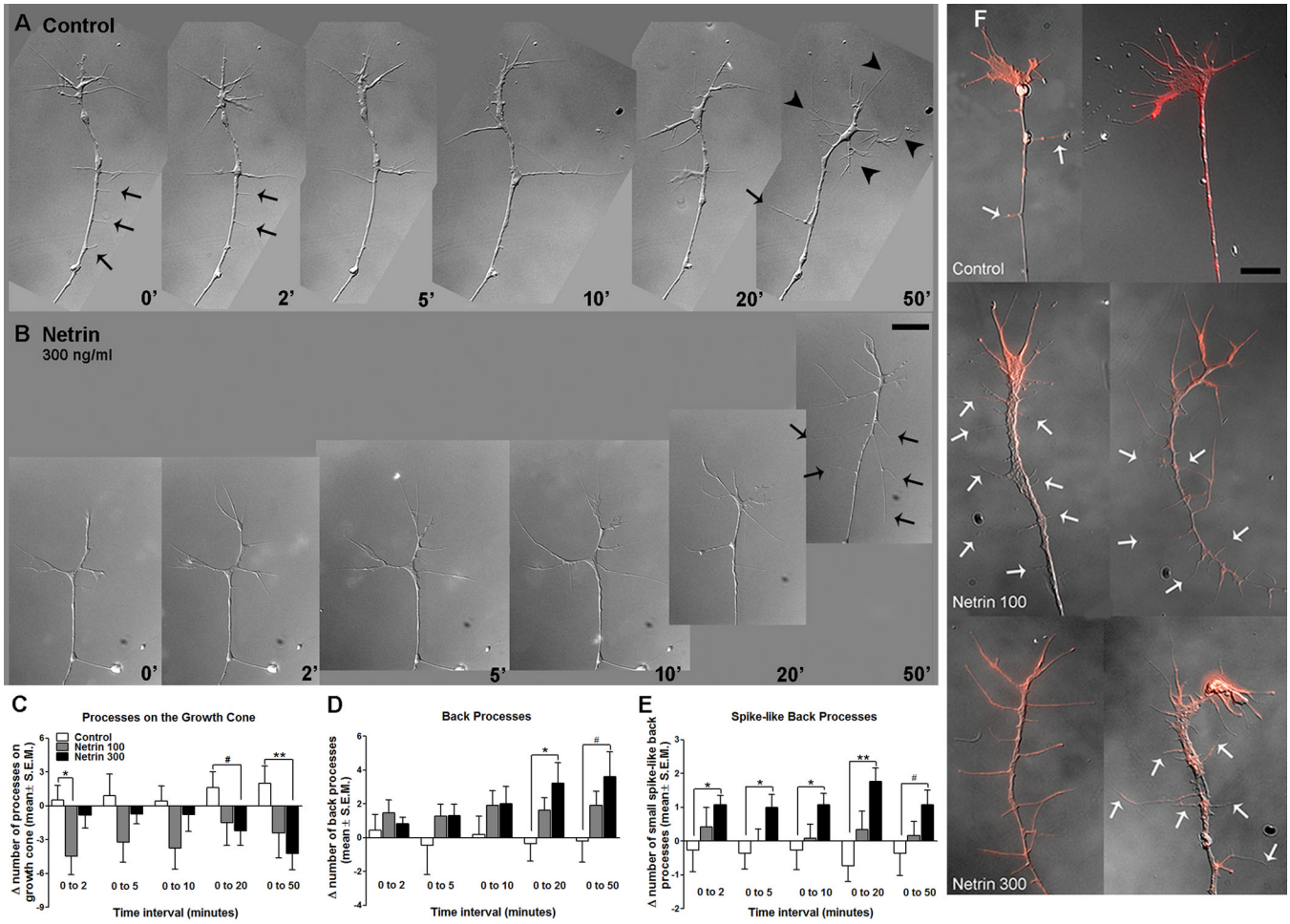

Figure 8. Netrin-1 induces extension of filopodial processes behind the growth cone in RGC axons in culture

A, B) Time-lapse sequence of sample RGC axon growth cones imaged in culture under control conditions (*A*) and following acute exposure to netrin-1 (*B*). Black arrowheads point to filopodial processes at the growth cone in ***A***, and arrows point to processes behind the growth cone in ***A*** and ***B***. These representative time-lapse images illustrate differences in the extension of filopodial processes in control and netrin-treated (300 ng/ml) growth cones. Scale bar, 10 μm. **C)** Quantitation of changes in number of filopodial processes at the growth cone show that netrin treatment results in growth cones with fewer growth cone processes than controls. **D, E)** The number of processes behind the growth cone, along the axon shaft (*D*; back processes), as well as the number of short, spike-like processes (less than 1.5 μm; *E*) behind the growth cone are increased after netrin treatment. **F)** Representative growth cones in fixed cultures one hour post-treatment, stained with rhodamine phalloidin (red), illustrate the decrease in the number of filopodial processes on the growth cone in RGC axons in cultures exposed to netrin. White arrows indicate back processes. Scale bar, 10 μm. *$p < 0.05$, and **$p < 0.005$. Error bars indicate SEM.

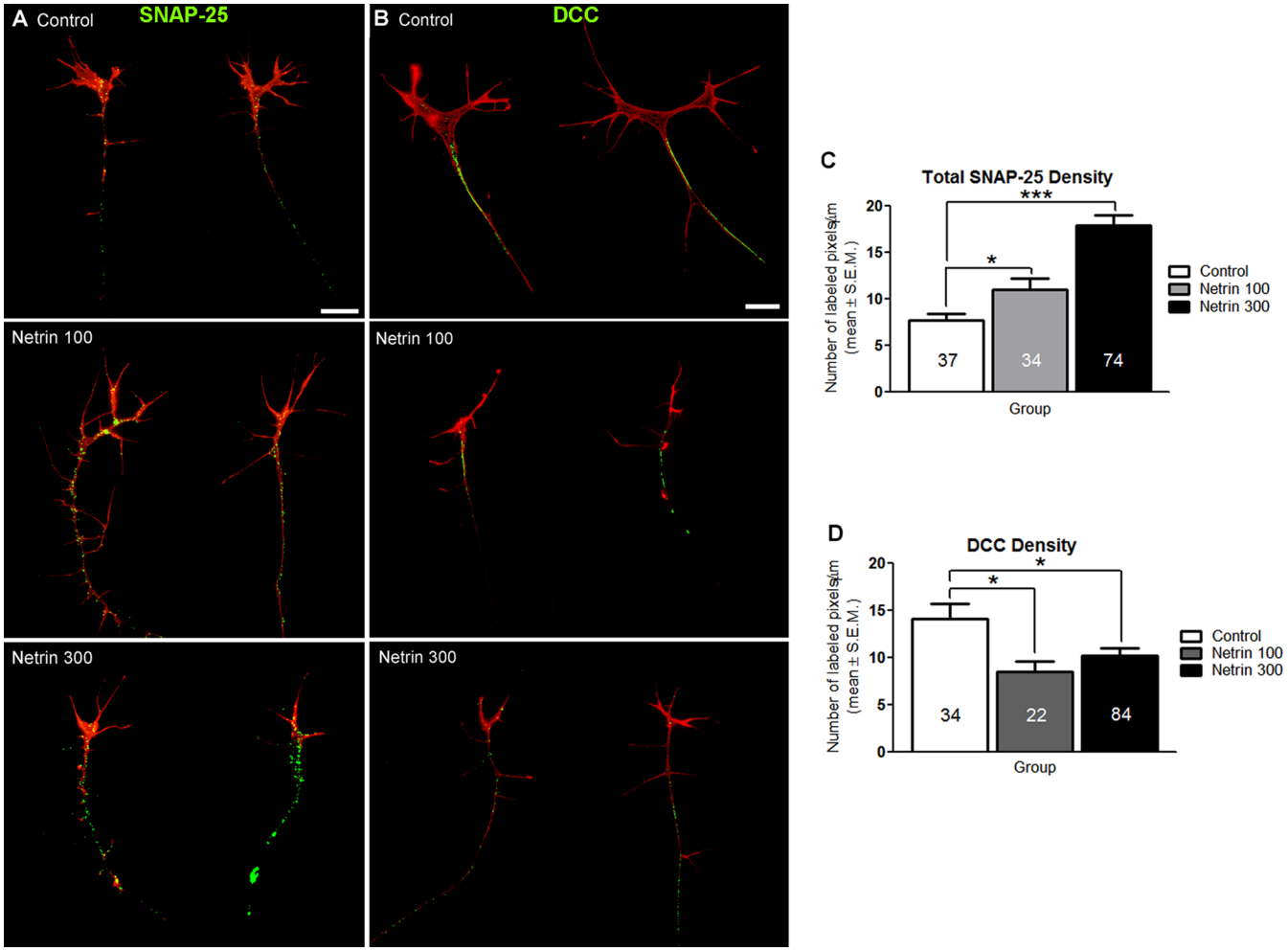

Figure 9. Acute exposure to netrin-1 influences presynaptic protein density and DCC expression in RGC axons in culture

A, B) Representative control and netrin-treated RGC growth cones in culture immunostained with antibodies to SNAP-25 (A, presynaptic protein marker) or antibodies to the netrin receptor DCC (B). Retinal explant cultures were grown in culture for 24 hours then treated with netrin-1(100 ng/ml or 300 ng/ml) or vehicle solution for 1 hour prior to fixation and immunostaining. Cultures were also stained with rhodamine phalloidin (red) prior to antibody staining to visualize the actin cytoskeleton. **A)** SNAP-25 immunoreactivity is observed throughout the axon shaft and at the growth cone in axons in control and netrin-treated cultures. Note that SNAP-25 immunoreactivity is increased by the netrin-1 treatment. Scale bar, 10 μm. **B)** DCC immunoreactivity is observed primarily along the axon, and is absent from growth cones in control and netrin-treated cultures. Dense DCC immunostaining was observed in axons of control cultures, but was reduced in axons from cultures treated with netrin-1 at the two concentrations used. Scale bar, 10 μm. **C)** The density SNAP-25 immunostaining was quantified by counting the number of immunoreactive pixels per total axon length (μm). A dose-dependent increase in the density of SNAP-25 immunostaining is observed in growth cones following netrin-1 treatment. **D)** Quantification of the density of DCC immunostaining along the axon showed that DCC levels decrease following exposure to netrin-1. Sample sizes are indicated by the numerical values inside bars. * signifies $p < 0.05$ and ***$p < 0.0005$. . Error bars indicate SEM.